Selecting the most appropriate time points to profile in high-throughput studies

Michael Kleyman*[1], Emre Sefer*[1], Teodora Nicola[2], Celia Espinoza[3], Divya Chhabra[3], James S. Hagood[3], Naftali Kaminski[4], Namasivayam Ambalavanan[2], Ziv-Bar Joseph[1]

*Equal contribution

1 Machine Learning and Computational Biology, School of Computer Science, Carnegie Mellon University, Pittsburgh, PA, USA

2 Division of Neonatology, Dept of Pediatrics, University of Alabama at Birmingham, Birmingham, AL, USA

3 Division of Respiratory Medicine, Dept of Pediatrics, University of California San Diego, La Jolla, CARady Children's Hospital San Diego, San Diego, CA

4 Section of Pulmonary, Critical Care and Sleep Medicine, School of Medicine, Yale University, New Heaven, CT

E-mail: zivbj@cs.cmu.edu

Abstract

Biological systems are increasingly being studied by high throughput profiling of molecular data over time. Determining the set of time points to sample in studies that profile several different types of molecular data is still challenging. Here we present the Time Point Selection (*TPS*) method that solves this combinatorial problem in a principled and practical way. *TPS* utilizes expression data from a small set of genes sampled at a high rate. As we show by applying *TPS* to study mouse lung development, the points selected by *TPS* can be used to reconstruct an accurate representation for the expression values of the non selected points. Further, even though the selection is only based on gene expression, these points are also appropriate for representing a much larger set of protein, miRNA and DNA methylation changes over time. *TPS* can thus serve as a key design strategy for high throughput time series experiments.

Supporting Website: `www.sb.cs.cmu.edu/TPS`

Introduction

Time series experiments are very commonly used to study a wide range of biological processes. Examples include various developmental processes [1], stem cell differentiation [2], immune responses [3], stress responses [4] and several others. Indeed, analysis of the largest repository of gene expression experiments, the Gene Expression Omnibus (GEO), determined that roughly a third of these datasets come from experiments profiling dynamic processes over time [5].

While mRNA gene expression data has been the primary source of high-throughput time series data, more recently several other genomic regulatory features are profiled over time. These include miRNA expression data [6], ChIP-Seq studied to determine TF targets [7] and several types of epigenetic markers including DNA methylation [8], histone modifications [9] and more. In fact, with the rise in our ability to perform such high-throughput time series analysis, many researchers are now combining a few or several of these time series profiling experiments in a single experiment [7,10] and then integrate theses datasets to obtain a better understanding of cellular activity.

While integrated analysis of high-throughput genomic datasets can greatly improve our ability to model biological processes and systems, it comes at a cost. From the monetary point of view, these costs include the increased number of Seq experiments required to profile all types of genomic features. While such costs are common to all types of studies utilizing high-throughput data, they can be prohibitively high for time series based studies since they are multiplied by the number of time points required, the number of repeats performed for each time point and the number of different types of data being profiled. Importantly, even if the budget is not an issue, the ability to obtain enough samples for profiling all genomic features at all time points may be challenging, if not completely prohibitive.

One of the key determinants of the experimental and sample acquisition costs associated with time series studies is the number of time points that are being profiled. In most studies, the first and last time point can usually be determined by the researcher (for example, the time from birth to full lung structural development and maturation in mice). However, the number of samples required between these two points and the sampling frequency (given a fixed budget) are often hard to determine based on phenotypic observations since the molecular events of interest may precede such phenotypic events. To date, sampling rates have largely been determined using one of two ad-hoc protocols. The first utilized uniform sampling across the duration of the study [11] with the number of samples constrained by the available budget and samples. The second relied on some (conceived or real) knowledge of the process, often based on phenotypic observations. These studies, especially for responses though also for development, have often used nonuniform sampling [6, 12] though it is hard to determine if such sampling misses important molecular events between the sampled points.

Relatively little work has focused so far on the selection of time points to sample in high

throughput time series studies. Singh et al [13] and Rosa et al [14] presented an iterative process which starts with profiling a small number of time points and then selects the next time point either based on an Active Learning method [13] or based on using prior related experiments [14]. Next the selected point is profiled and the process is repeated until a stopping criteria has been reached. Both of these methods require several iterations until the final time series is profiled, which can drastically lengthen the experiment time and can introduce additional biases making them less useful in practice. In addition, these methods employ a stopping criteria that does not take into account the full profile and also require that related time series expression experiments be used to select the point, which may be problematic when studying new processes or treatments.

Here, we propose the first non iterative method to address the issue of sampling rates across all different genomic data types. Our method starts by selecting a small set of genes that are known to be associated with the process being studied (while the full set is often unknown, for most processes a small set is usually known in advance). Next, we use a cheap array-based technology to sample these genes at a high, uniform rate across the duration of the study. Note that unlike standard curve fitting algorithms, a method for selecting time points for these experiments is required to accommodate over a hundred curves (for all genes) simultaneously and we discuss various ways to formulate this as an optimization problem. To solve these optimization problems, we developed the Time Points Selection method (*TPS*), an algorithm that uses spline based analysis and combinatorial search to select a subset of the points that, when combined, provide enough information for reconstructing the values for all genes across all time points. The number of points selected can either be set in advance by the user (for example, based on budget constraints) or can be defined as a function of the reconstruction error. The selected time points are then used for the larger, genomewide experiments across the different types of data being profiled.

To test and evaluate the method we applied it to study lung development in mice. Normal development of lung alveoli through the process of alveolar septation is a dynamic, coordinated process that requires the accurate spatial and temporal integration of signals. We currently lack a comprehensive understanding of the dynamic networks that govern normal alveolar septation. Thus, lung development can serve as an ideal test case for TPS since a variety of different time series genomic datasets are needed to enable accurate reconstruction of networks regulating this process. As we show, *TPS* was able to successfully identify time points for reconstructing the mRNA profiles of selected genes and these points improved upon uniform based sampling for such points. Further, we show that the set of points selected based on the analysis of this limited set of highly sampled mRNAs is also appropriate for sampling a much larger, unbiased, set of miRNA profiles as well as to determine the temporal protein levels of over 1000 proteins. Finally, we show that the mRNA samples can also be used to determine the optimal sampling points for a DNA methylation study of the same developmental process.

Results

The Time Points Selection (*TPS*) method

We developed *TPS* to select a subset of k time points from an initial larger set of n points such that the selected subset provides an accurate, yet compact, representation of the temporal trajectory. Figure 1 presents an overview of the method. *TPS* utilizes splines to represent temporal profiles and implements a cross-validation strategy to evaluate potential sets of points. Following initialization which is based on the expression values, we employ a greedy search procedure that adds and removes points until a local minima is reached (Methods). The resulting set is then used for the larger genomic and epigenetic experiments.

To test the usefulness of *TPS*, we used it to determine time points for a lung development study in mice. We first profiled the expression of 126 genes known or suspected to be involved in lung development using NanoString (See Appendix Methods for a list of the selected genes and the reason each was selected). We then used *TPS* analysis of these experiments to select a subset of time points for profiling the expression of a larger, unbiased, set of miRNAs. Finally, we have used *TPS* to design time series experiments to study DNA methylation patterns for a subset of the genes.

TPS identifies subset of important time points across multiple genes

We have tested the performance of *TPS* by using it to select subsets of points ranging from 3 to 25 and evaluating how well these can be used to determine the values of non-sampled points. To determine the accuracy of the reconstructed profiles using the selected points, we computed the average mean squared error for points that were not used by the method (Methods). The results are presented in Figure 2. The figure includes a comparison of our method with two baseline methods: a random selection of the same number of points and uniform sampling of points within the range being studied, a method that is commonly used for time series expression profiling as discussed above. We have also compared the performance of the different strategies for initializing the set of points as discussed in Method (sorting by absolute differences or by equal partition) and between different methods for searching for the optimal subset (simulated annealing, weighting genes by cluster size, and adding/removing multiple time points per iteration, Methods). Finally, the figure also presents the repeat noise values which is the theoretical limit for the performance of any profile reconstruction method.

As expected, we find significant performance improvement when using *TPS* when compared to randomly selected points. Importantly, we also see a significant and consistent improvement (for all sizes of selected time points) over uniform sampling highlighting the advantage of condition specific sampling decisions. Sorting initial points by absolute values further improves the performance

highlighting the importance of initialization when searching large combinatorial spaces. Simulated annealing, weighting, and multiple point selection improve performance as well. As the number of points used by *TPS* increases, it leads to results that are very close to the error represented by noise in the data (0.108) (Figure 2 - figure supplement 1).

Figure 3 presents the reconstructed and measured expression values when using *TPS* to select 13 time points (less than a third of the points that were profiled). Note that even though each of these genes has distinct trajectory and inflection points, the selected set of time points enable *TPS* to fit all quite accurately without overfitting (See Figure 4 - figure supplement 2 for figures of several other genes and for figures reconstructed by using the best 8 time points as determined by *TPS*, respectively).

Identified time points using mRNA data are appropriate for miRNA profiling

To test the usefulness of our method for predicting the correct sampling rates for other genomic datasets, we next profiled mouse miRNAs for the same developmental process. miRNAs have been known to regulate lung development [15] and several miRNAs are differentially expressed during this developmental process [16]. Several of these are also coordinately activated with various TFs to control specific transitions during development [6]. Thus, any large scale effort to model lung development would require the profiling of miRNAs as well. Unlike the mRNA dataset, which utilized prior knowledge to profile less than 1% of all genes, the miRNA dataset contained a much larger number of miRNAs ($\tilde{6}00$). Thus, the miRNA data represents an unbiased sample providing information on whether using one type of genomic data can be helpful for determining rates for other types. In our analysis, we normalized miRNA values by variance mean normalization [17].

To test *TPS* on this dataset, we used the *mRNA* expression data to select time points and then used the miRNA expression values for the selected time points to reconstruct the complete trajectories for each miRNA. The results are presented in Figure 4. As can be seen, when using the points selected based on the mRNA data we achieve a much lower error when compared to the error resulting from using the same number of uniform or random points ($p < 0.01$ for random based on randomization analysis) highlighting the relationship between the two datasets and the ability to use one to determine points for the other. More generally, even though the noise in the miRNA data is higher than for the mRNA dataset, relative ordering of the performance of each of the methods is similar to the mRNA results in Figure 2. This serves as a strong indication that mRNAs can serve as a general proxy for selecting time points for other genomic datasets. Figure 4 - supplementary figure 4 presents the error achieved when using the miRNA data itself to select the set of points (evaluated on the miRNA data). As expected, the performance when using the miRNA data itself is better than when using the mRNA data. However, when taking into account the inherent noise in the data the differences are not large. For example, when using the 13 selected

mRNA points, the average mean squared error is 0.4312 whereas when using the optimal points based on the miRNA data itself the error is 0.4042.

Figure 4 - figure supplement 2 presents the reconstructed and measured expression values for a few miRNAs based on time points identified using the mRNA dataset. As with the mRNA data, the ability to accurately reconstruct different miRNA profiles highlights the importance of selecting a global set of points that can fit all genes and miRNAs in our study.

We have also analyzed the performance of *TPS* when using the mRNA data to select sampling time points for profiling the levels of more than 1000 proteins. we observed results that are very simila to the results obtained for the miRNA time point selection. Specifically, the points selected by TPS lead to reconstruction errors that are lower than those observed for uniform sampling or for a random set of the same number of points further deminstrating the general applicability of our method. See Appendix Results for details.

Using *TPS* to select time points for DNA Methylation analysis

In addition to mRNA and miRNA expression data, epigenetic data has been increasingly studied in time series experiments [18,19]. To test the ability of the mRNA data to determine appropriate points for DNA methylation analysis, we used targeted bisulfite sequencing to profile three CpG-enriched regions for 13 genes at 8 of the 42 time points used for the mRNA and miRNA studies (Methods). We next applied *TPS* to the mRNA data of these 8 points to select the best subest of 4 points and compared the selected points to those that would have been selected using the methylation data itself. The 4 points identified using the mRNA data (0.5, 5, 15, 26) were exactly the same as the ones selected using the methylation data indicating again that mRNA data is a good proxy for the dynamics of the epigenetic data as well. Figure 5 - figure supplement 1 presents the reconstructed splines over the identified points for several genomic methylation loci. Figure 5 presents the methylation and expression curves for 3 genes: *Akt,1 Cdh11*, and *Tnc*. These were the genes with the strongest negative correlation between their methylation and expression. As can be seen, in several cases we observed strong negative or positive correlations between the two datasets in the time points we used serving as another indication for the ability to use one dataset to select the sampling points for the other. See Figure 5 - figure appendix 2 for correlation of all genes.

Discussion

Time series gene expression experiments are widely used in several studies. More recently, advances in sequencing and proteomics are enabling the profiling of several other types of genomic data over time. Here we focused on lung development in mice with the goal of identifying an optimal set of time points for profiling various genomic and proteomic data types for this process.

An important question is whether a better selection of time points really leads to observations that are missed when using an inferior set of points (even if the number of points is the same)? To answer this question we looked at several prior studies that profiled mouse lung development over time using various high throughput assays. Table 1 presents 9 representative studies and lists the biological data that was profiled and the time points that were used. As can be seen, while certain time points seem to be widely used across studies (for example, 7d) others were profiled in only one or two of the studies (2d, 10d, three weeks). This raises several issues. First, it is very hard to compare or combine these datasets (for example, protein levels were not profiled on day 7 [20] whereas all mRNA levels were). It also makes it hard to determine if differences between DE genes or miRNAs between these studies are the result of differences in the underlying conditions studied (for example, when testing for mutants or treatments) or simply the result of different sampling. Finally, each of these studies may have missed key genes, proteins or miRNAs because of the sampling used restricting the ability of downstream analysis to use the data to model causal and regulatory events in lung development.

To illustrate these problems we compared the resulting curves using three of the sampling rates from Table 1 to the reconstructed curves obtained by using *TPS* to select the optimal 5 and 8 time points. For example, the points selected by [6] are 0, 4, 7, 14 and 28 (since 28 is last day in our analysis we used it instead of 42). In contrast, *TPS* selects 0.5, 6, 9.5, 19 and 28. As can be seen in Figure 6, important expression changes in key genes are missed by using the arbitrary points while the *TPS* points are able to correctly reconstruct these profiles even though the total number of points is the same (5). More globally, the error for the arbitrary set of selected points is much higher on average (Appendix Table 4). Similar results are obtained for the other sampling rates used in the past (Figure 6, Appendix Table 4) and when comparing TPS to iterative methods previously suggested for selecting the set of points to profile (Figure 1 Figure supplement 1). This indicates that accurate selection of time points can have a large impact on the ability of the study to identify key genes and events. See also Appendix Results for a discussion about the importance of the differences between the TPS and prior work results for selected genes.

Our method relies on a very small subset of genes that are known to be involved in the process studied for the initial (highly sampled) set of experiments. While such set is known for several processes, there may be cases where very little is known about the biological process and so it may be hard to obtain such set. TPS can still be applied to determine sampling rates for such processes

using a small *random* set of genes. To illustrate this we repeated the analysis presented in Results using only the measured values of 25% of genes in our original set and replacing the values for the other genes with random profiles. As we show in Figure 2 - figure supplement 3, even when using such set, the time points selected by TPS greatly improve upon an arbitrary set of the same number of time points. Since in most time series experiments at least 25% of the genes are differnetially expressed (and in several cases a much larger fraction, [21, 22] a random selection of genes is likely to exhibit similar results even for poorly understood processes.

Beyond the analysis of a specific type of data, several studies have now been profiling multiple types of genomic data over time. Such studies need to agree on a set of time points which would be common to all experiments so that these diverse types can be integrated to form a unified model [1, 7]. To date, the selection of such points relied on ad-hoc methods. The processes being studied were either sampled uniformly or based on prior knowledge. However, known properties of such systems were often been based on phenotypic observations which may not necessarily agree with the timing of molecular events. In addition, in many cases studies of the same, or similar processes differed with respect to the time points that have been profiled. For example, early work on the analysis of cell cycle data in yeast utilized both uniform and nonuniform sampling [23] and recent studies of circadian rhythms have followed a similar pattern [24, 25]. Similarly, more recent analysis of responses to flu diverged widely in the (nonuniform) sampling rates that were used [26, 27].

TPS addresses these problems by using a principled method for determining sampling rates. An important goal in the development of *TPS* was to enable it to be successfully applied to different types of biological datasets. As we show, a relatively inexpensive, gene centric, method provides a very good solution for RNA expression profiling as well as other types of data including miRNAs and DNA methylation. Thus, a combined experiment can be fully designed using our method.

While we evaluated TPS on several types of high throughput data, we have only tested it so far on data for a specific biological process (lung development in mice). While we believe that such data is both challenging and representative and thus provides a good test case for the method, analysis of additional datasets may identify new challenges that we have not addressed and we leave it to future work to address these.

TPS, including all initialization methods discussed, is implemented in Python and is available on the supporting website. We hope that as sequencing technology continues to advance, more and more studies would integrate diverse types of time series data and will utilize *TPS* in the design pipeline of their studies.

Materials and Methods

mRNA and miRNA used in the study

To select the list of 126 genes used in the NanoString profiling we searched the literature for genes that have been linked to the following processes: (a) Cell type specification genes (e.g. alveolar type I epithelial, alveolar type II epithelial, any epithelial, basal, endothelial, mesenchymal, pericyte, fibroblast, monocyte), (b) genes known to be up or down regulated during septation, (c) genes known to be altered in DNA methylation during development, (d) genes known to be involved in septation, (e) genes known to be regulated by miRNA involved in septation, and (f) genes known to be regulated by DNA methylation during fibrosis. Appendix Table 1 contains a list of the selected genes and the process for which they were selected.

For the miRNA set we used a commercially available, unbiased, array (the nCounter Mouse miRNA Expression Assay Kit, NanoString).

mRNA and miRNA profiling and analysis

A total of 240 samples were isolated by Laser Capture Microscopy (LCM) from murine lung at multiple time points (E16.5, P.05 to P14 every 12h, and P15 to P28 every 24h). The samples were used to prepare total RNA. RNA extraction was performed by miRNeasy MicroKit (Qiagen) following the manufacturers protocol. RNA concentration and integrity were measured by using NanoDrop ND-2000 and 2200 Tape Station. A custom NanoString probe set (Reporter Code set and Capture Probe set) for 126 genes was designed and the nCounter Gene Expression Assay was performed using 50 ng total RNA. The data files produced by the nCounter Digital Analyzer were exported as a Reporter Code Count (RCC) file and data normalization was performed using the nSolver, the analysis software provided by Nanostring.

DNA Methylation analysis

Mouse alveolar lung tissues attached to LCM caps were stored at -80oC until processing. DNA was extracted using the ZR Genomic DNA-Tissue MicroPrep kit (Zymo Research). Incubation with Digestion buffer and proteinase K was done overnight at 55C in inverted tubes. 13 genes were chosen for targeted NextGen bisulfite sequencing (NGBS): *Igfbp3, Wif1, Cdh11, Eln, Sox9, Tnc, Dnmt3a, Akt, Vegfa, Lox, Foxf2, Zfp536* and *Src*, based on published data [28]. Targeted NGBS was done on samples collected at: E16.5, E18.5, P0.5, P1.5, P2.5, P5, P10, P15, P19 and P26. Multiplex PCR was performed using 0.5 units of TaKaRa EpiTaq HS (Takara Bio) in 2x master mix. FASTQ files were aligned using open source Bismark Bisulfite Read Mapper using Bowtie2. Methylation levels were calculated in Bismark. Sites where the difference in methylation was less than 5% over the entire time period, those where there was a difference of $> 20\%$ at a single time point and those with less than 3 non zero values were removed from the analyses.

Problem statement

Our goal is to identify a (small) subset of time points that can be used to accurately reconstruct the expression trajectory for *all* genes or other molecules being profiled. We assume that we can efficiently and cheaply obtain a dense sample for the expression of a very small subset of representative genes (here we use nanostring to profile less than 0.5% of all genes) and attempt to use this subset to determine optimal sampling points for the entire set of genes.

Formally, let G be the set of genes we have profiled in our dense sample, $T = \{t_1, t_2, \ldots, t_T\}$ be the set of all sampled time points. We assume that for each time point we have R repeats for all genes. We denote by e^r_{gt} be the expression value for gene $g \in G$ at time $t \in T$ in the r'th repeat for that time point. We define $D_g = \{e^r_{gt}\,, t \in T, r \in R$ as the complete data for gene g over all replicates and time points T.

To constrain the set of points we select, we assume that we have a predefined budget k for the maximum number of time points we can sample in the complete experiment (i.e. for profiling all genes, miRNAs, epigenetic marks etc. using high-throughput seq experiments). We are interested in selecting k time points from T which, when using only the data collected at these k points, minimizes the prediction error for the expression values of the unused points. To evaluate such a selection, we use the selected values to obtain a smoothing spline [12, 29, 30] function for each gene and compare the predicted values based on the spline to the measured value for the non-selected points to determine the error. In our problem, t_1 and t_T define the first and end points, so they are always selected. The rest of the points are selected to maximize the following objective 1:

Problem 1. *Given D_g for genes $g \in G$, the number of desired time points k, identify a subset of $k-2$ time points in $T \setminus \{t_1, t_T\}$ which minimizes the prediction error for the expression values of all genes in the remaining time points.*

Spline assignments

Before discussing the actual procedure we use to select the set of time points, we discuss the method we use to assign splines based on a selected subset of points for each gene. There are two issues that needs to be resolved when assigning such smoothing splines: 1. The number of knots (control points) and 2. their spacing. Past approaches for using splines to model time series gene expression data have usually used the same number of control points for all genes regardless of their trajectories [31, 32], and mostly employed uniform knot placements. However, since our method needs to be able to adapt to any size of k as defined above, we attempt to also select the number of knots and their spacing. We do this by using a regularization parameter for the fitted cubic smoothing spline where number of knots is increased until the smoothing condition is satisfied [30]. Regularization parameter is estimated by leave-one-out cross-validation (LOOCV).

TPS: Iterative process to select points

Because of the highly combinatorial nature of the time points, we rely on a greedy iterative process to select the optimal points as summarized in Figure 1 (See Appendix Methods for pseudocode).

There are three key steps in this algorithm which we discuss in detail below.

- *Selecting the initial set of points:* When using an iterative algorithm to solve non-convex problems with several local minima, a key issue is the appropriate selection of the initial solution set [33,34]. We have tested a number of methods for performing such initializations and results for some of these are presented in Figure 1 - figure supplement 2. Since the goal of the method is to optimize a specific function (error on the left out set of expression values measured at time points not used), all initialization methods can be tested for each dataset and the solution minimizing the left out error can be used. See Appendix Methods for details.

- *Iterative improvement step:* After selecting the initial set, we begin the iterative process of refining the subset of selected points. In this step we repeat the following analysis in each iteration. We exhaustively remove all points from the existing solution (one at a time) and replace it with all points that were not in the selected set (again, one at a time). For each pair of such point, we compute the error resulting from the change (using the splines computed based on the current set of points evaluated on the left out time points), and determine if the new point reduces the error or not. Formally, let $T^- = T \setminus \{t_1, t_T\}$ and C_n be set of points for iteration n. We are interested in finding a point pair $(t_a \in C_n, t_b \in T^- \setminus C_n)$ which minimizes the following error ratio for the next iteration $C_{n+} = C_n \setminus \{t_a\} \cup \{t_b\}$:

$$error\ ratio = \frac{error(C_{n+})}{error(C_n)} = \frac{\sum_{g \in G} \sum_{r \in R} \sum_{t \in T \setminus C_{n+}} (\hat{e}_{gt}^{C_{n+}} - e_{gt}^{r})^2}{\sum_{g \in G} \sum_{r \in R} \sum_{t \in T \setminus C_n} (\hat{e}_{gt}^{C_n} - e_{gt}^{r})^2} \quad (1)$$

  where $\hat{e}_{gt}^{C_n}$ is our spline based estimate of the expression of gene g at time t by fitting smoothing spline over points C_n. If there are pairs which lead to an error ratio of less than 1 in the above function, we select the best (lowest error), assign it to C_{n+1} and continue the iterative process. Otherwise we terminate the process and output C_n as the optimal solution. While the process is guaranteed to converge, given the large combinatorial search space convergence can be slow. This makes adequate initialization an important issue which we have focused on. In practice we find that the search usually converges very fast (within 10-15 iterations).

- *Fitting smoothing spline:* The third key step of our approach is fitting a smoothing spline to every gene independently for the selected subset of time points. As discussed above, this is done by using a regularized version of approximating splines which allow us to determine a unique number of control points and spacing for each of the genes. See Appendix Methods for more details.

Individual vs. Cluster based Evaluation

So far, we assumed that error of each gene has same contribution to the overall error. However, this assumption ignores the fact that expression profiles of genes are correlated with the expression of other genes. To take the correlation between gene profiles into account, we also performed cluster based evaluation of genes where we analyzed the error by weighting each gene in terms of inverse of the numbers of genes in the cluster it belongs. This scheme ensures that each cluster contributes equally to the resulting error rather than each gene. We find clusters by k-means algorithm over time series-data by treating each gene as a point in R^T space as well as over a vector of randomly sampled T time points on fitted spline [35]. We use Bayesian Information Criterion (BIC) to determine the optimal number of clusters [36].

Acknowledgment

We thank the the LungMAP consortium for useful comments regarding the methods and analysis presented in this paper. Work supported in part by NIH grant U01 HL122626.

References

[1] Sushmita Roy, Jason Ernst, Peter V Kharchenko, Pouya Kheradpour, Nicolas Negre, Matthew L Eaton, Jane M Landolin, Christopher A Bristow, Lijia Ma, Michael F Lin, et al. Identification of functional elements and regulatory circuits by drosophila modencode. *Science*, 330(6012):1787–1797, 2010.

[2] Jamie M Sperger, Xin Chen, Jonathan S Draper, Jessica E Antosiewicz, Chris H Chon, Sunita B Jones, James D Brooks, Peter W Andrews, Patrick O Brown, and James A Thomson. Gene expression patterns in human embryonic stem cells and human pluripotent germ cell tumors. *Proceedings of the National Academy of Sciences*, 100(23):13350–13355, 2003.

[3] Nir Yosef and Aviv Regev. Impulse control: temporal dynamics in gene transcription. *Cell*, 144(6):886–896, 2011.

[4] Anthony Gitter, Miri Carmi, Naama Barkai, and Ziv Bar-Joseph. Linking the signaling cascades and dynamic regulatory networks controlling stress responses. *Genome research*, 23(2):365–376, 2013.

[5] Guy E Zinman, Shoshana Naiman, Yariv Kanfi, Haim Cohen, and Ziv Bar-Joseph. Expressionblast: mining large, unstructured expression databases. *Nature methods*, 10(10):925–926, 2013.

[6] Marcel H Schulz, Kusum V Pandit, Christian L Lino Cardenas, Namasivayam Ambalavanan, Naftali Kaminski, and Ziv Bar-Joseph. Reconstructing dynamic microrna-regulated interaction networks. *Proceedings of the National Academy of Sciences*, 110(39):15686–15691, 2013.

[7] Katherine Noelani Chang, Shan Zhong, Matthew T Weirauch, Gary Hon, Mattia Pelizzola, Hai Li, Shao-shan Carol Huang, Robert J Schmitz, Mark A Urich, Dwight Kuo, et al. Temporal transcriptional response to ethylene gas drives growth hormone cross-regulation in arabidopsis. *Elife*, 2:e00675, 2013.

[8] Zakary S Singer, John Yong, Julia Tischler, Jamie A Hackett, Alphan Altinok, M Azim Surani, Long Cai, and Michael B Elowitz. Dynamic heterogeneity and dna methylation in embryonic stem cells. *Molecular cell*, 55(2):319–331, 2014.

[9] Sharon L Paige, Sean Thomas, Cristi L Stoick-Cooper, Hao Wang, Lisa Maves, Richard Sandstrom, Lil Pabon, Hans Reinecke, Gabriel Pratt, Gordon Keller, et al. A temporal chromatin signature in human embryonic stem cells identifies regulators of cardiac development. *Cell*, 151(1):221–232, 2012.

[10] Jason D Buenrostro, Beijing Wu, Ulrike M Litzenburger, Dave Ruff, Michael L Gonzales, Michael P Snyder, Howard Y Chang, and William J Greenleaf. Single-cell chromatin accessibility reveals principles of regulatory variation. *Nature*, 523(7561):486–490, 2015.

[11] Jun Z Li, Blynn G Bunney, Fan Meng, Megan H Hagenauer, David M Walsh, Marquis P Vawter, Simon J Evans, Prabhakara V Choudary, Preston Cartagena, Jack D Barchas, et al. Circadian patterns of gene expression in the human brain and disruption in major depressive disorder. *Proceedings of the National Academy of Sciences*, 110(24):9950–9955, 2013.

[12] Ziv Bar-Joseph, Georg K Gerber, David K Gifford, Tommi S Jaakkola, and Itamar Simon. Continuous representations of time-series gene expression data. *Journal of Computational Biology*, 10(3-4):341–356, 2003.

[13] Rohit Singh, Nathan Palmer, David Gifford, Bonnie Berger, and Ziv Bar-Joseph. Active learning for sampling in time-series experiments with application to gene expression analysis. In *Proceedings of the 22nd international conference on Machine learning*, pages 832–839. ACM, 2005.

[14] Bruce A Rosa, Ji Zhang, Ian T Major, Wensheng Qin, and Jin Chen. Optimal timepoint sampling in high-throughput gene expression experiments. *Bioinformatics*, 28(21):2773–2781, 2012.

[15] Roberto Sessa and Akiko Hata. Role of micrornas in lung development and pulmonary diseases. *Pulmonary circulation*, 3(2):315, 2013.

[16] Andrew E Williams, Sterghios A Moschos, Mark M Perry, Peter J Barnes, and Mark A Lindsay. Maternally imprinted micrornas are differentially expressed during mouse and human lung development. *Developmental Dynamics*, 236(2):572–580, 2007.

[17] Benjamin M Bolstad, Rafael A Irizarry, Magnus Åstrand, and Terence P. Speed. A comparison of normalization methods for high density oligonucleotide array data based on variance and bias. *Bioinformatics*, 19(2):185–193, 2003.

[18] Rudolf P Talens, Dorret I Boomsma, Elmar W Tobi, Dennis Kremer, J Wouter Jukema, Gonneke Willemsen, Hein Putter, P Eline Slagboom, and Bastiaan T Heijmans. Variation, patterns, and temporal stability of dna methylation: considerations for epigenetic epidemiology. *The FASEB Journal*, 24(9):3135–3144, 2010.

[19] Eberhard Schneider, Galyna Pliushch, Nady El Hajj, Danuta Galetzka, Alexander Puhl, Martin Schorsch, Katrin Frauenknecht, Thomas Riepert, Achim Tresch, Annette M Müller, et al. Spatial, temporal and interindividual epigenetic variation of functionally important dna methylation patterns. *Nucleic acids research*, 38(12):3880–3890, 2010.

[20] Brian Cox, Thomas Kislinger, Dennis A Wigle, Anitha Kannan, Kevin Brown, Tadashi Okubo, Brigid Hogan, Igor Jurisica, Brendan Frey, Janet Rossant, et al. Integrated proteomic and transcriptomic profiling of mouse lung development and nmyc target genes. *Molecular systems biology*, 3(1):109, 2007.

[21] Lecong Zhou, Santiago X Mideros, Lei Bao, Regina Hanlon, Felipe D Arredondo, Sucheta Tripathy, Konstantinos Krampis, Adam Jerauld, Clive Evans, Steven K St Martin, et al. Infection and genotype remodel the entire soybean transcriptome. *BMC genomics*, 10(1):1, 2009.

[22] Wei Shi, Yang Liao, Simon N Willis, Nadine Taubenheim, Michael Inouye, David M Tarlinton, Gordon K Smyth, Philip D Hodgkin, Stephen L Nutt, and Lynn M Corcoran. Transcriptional profiling of mouse b cell terminal differentiation defines a signature for antibody-secreting plasma cells. *Nature immunology*, 16(6):663–673, 2015.

[23] Paul T Spellman, Gavin Sherlock, Michael Q Zhang, Vishwanath R Iyer, Kirk Anders, Michael B Eisen, Patrick O Brown, David Botstein, and Bruce Futcher. Comprehensive identification of cell cycle–regulated genes of the yeast saccharomyces cerevisiae by microarray hybridization. *Molecular biology of the cell*, 9(12):3273–3297, 1998.

[24] Kai-Florian Storch, Ovidiu Lipan, Igor Leykin, N Viswanathan, Fred C Davis, Wing H Wong, and Charles J Weitz. Extensive and divergent circadian gene expression in liver and heart. *Nature*, 417(6884):78–83, 2002.

[25] Hiroki R Ueda, Wenbin Chen, Akihito Adachi, Hisanori Wakamatsu, Satoko Hayashi, Tomohiro Takasugi, Mamoru Nagano, Ken-ichi Nakahama, Yutaka Suzuki, Sumio Sugano, et al. A transcription factor response element for gene expression during circadian night. *Nature*, 418(6897):534–539, 2002.

[26] Sagi D Shapira, Irit Gat-Viks, Bennett OV Shum, Amelie Dricot, Marciela M de Grace, Liguo Wu, Piyush B Gupta, Tong Hao, Serena J Silver, David E Root, et al. A physical and regulatory map of host-influenza interactions reveals pathways in h1n1 infection. *Cell*, 139(7):1255–1267, 2009.

[27] Chengjun Li, Armand Bankhead, Amie J Eisfeld, Yasuko Hatta, Sophia Jeng, Jean H Chang, Lauri D Aicher, Sean Proll, Amy L Ellis, G Lynn Law, et al. Host regulatory network response to infection with highly pathogenic h5n1 avian influenza virus. *Journal of virology*, 85(21):10955–10967, 2011.

[28] Alain Cuna, Brian Halloran, Ona Faye-Petersen, David Kelly, David K Crossman, Xiangqin Cui, Kusum Pandit, Naftali Kaminski, Soumyaroop Bhattacharya, Ausaf Ahmad, et al. Al-

terations in gene expression and dna methylation during murine and human lung alveolar septation. *American journal of respiratory cell and molecular biology*, (ja), 2014.

[29] Carl De Boor. A practical guide to splines. *Mathematics of Computation*, 1978.

[30] Grace Wahba. *Spline models for observational data*, volume 59. Siam, 1990.

[31] Numanul Subhani, Luis Rueda, Alioune Ngom, and Conrad J Burden. Multiple gene expression profile alignment for microarray time-series data clustering. *Bioinformatics*, 26(18):2281–2288, 2010.

[32] Ziv Bar-Joseph, Georg Gerber, Itamar Simon, David K Gifford, and Tommi S Jaakkola. Comparing the continuous representation of time-series expression profiles to identify differentially expressed genes. *Proceedings of the National Academy of Sciences*, 100(18):10146–10151, 2003.

[33] John A Hartigan. *Clustering algorithms*. John Wiley & Sons, Inc., 1975.

[34] Geoffrey McLachlan and David Peel. *Finite mixture models*. John Wiley & Sons, 2004.

[35] Christopher M Bishop. *Pattern recognition and machine learning*. springer, 2006.

[36] Gideon Schwarz et al. Estimating the dimension of a model. *The annals of statistics*, 6(2):461–464, 1978.

[37] AE Bonner, WJ Lemon, and M You. Gene expression signatures identify novel regulatory pathways during murine lung development: implications for lung tumorigenesis. *Journal of medical genetics*, 40(6):408–417, 2003.

[38] Erik Melén, Alvin T Kho, Sunita Sharma, Roger Gaedigk, J Steven Leeder, Thomas J Mariani, Vincent J Carey, Scott T Weiss, and Kelan G Tantisira. Expression analysis of asthma candidate genes during human and murine lung development. *Respir Res*, 12(1):86, 2011.

[39] Manoj Bhaskaran, Yang Wang, Honghao Zhang, Tingting Weng, Pradyumna Baviskar, Yujie Guo, Deming Gou, and Lin Liu. Microrna-127 modulates fetal lung development. *Physiological genomics*, 37(3):268–278, 2009.

[40] Jie Dong, Shari Sutor, Guoqian Jiang, Yajun Cao, Yan W Asmann, and Dennis A Wigle. c-myc regulates self-renewal in bronchoalveolar stem cells. *PloS one*, 6(8):e23707, 2011.

[41] Meredith Cormack, Miao Lin, Alexey Fedulov, Steve J Mentzer, and Akira Tsuda. Age-dependent changes in gene expression profiles of postnatally developing rat lungs exposed to nano-size and micro-size cuo particles. *The FASEB Journal*, 24(1_MeetingAbstracts):612–18, 2010.

[42] Edward M Mager, Gabriele Renzetti, Alexander Auais, and Giovanni Piedimonte. Growth factors gene expression in the developing lung. *Acta paediatrica*, 96(7):1015–1020, 2007.

[43] Thomas J Mariani, Jeremy J Reed, and Steven D Shapiro. Expression profiling of the developing mouse lung: insights into the establishment of the extracellular matrix. *American journal of respiratory cell and molecular biology*, 26(5):541–548, 2002.

[44] Daiya Takai and Peter A Jones. Comprehensive analysis of cpg islands in human chromosomes 21 and 22. *Proceedings of the national academy of sciences*, 99(6):3740–3745, 2002.

[45] Peter Rice, Ian Longden, Alan Bleasby, et al. Emboss: the european molecular biology open software suite. *Trends in genetics*, 16(6):276–277, 2000.

[46] Scott Kirkpatrick, C Daniel Gelatt, Mario P Vecchi, et al. Optimization by simulated annealing. *science*, 220(4598):671–680, 1983.

[47] Christian H Reinsch. Smoothing by spline functions. *Numerische mathematik*, 10(3):177–183, 1967.

[48] Martin Guilliams, Ismé De Kleer, Sandrine Henri, Sijranke Post, Leen Vanhoutte, Sofie De Prijck, Kim Deswarte, Bernard Malissen, Hamida Hammad, and Bart N Lambrecht. Alveolar macrophages develop from fetal monocytes that differentiate into long-lived cells in the first week of life via gm-csf. *The Journal of experimental medicine*, 210(10):1977–1992, 2013.

[49] Vikram Agarwal, George W Bell, Jin-Wu Nam, and David P Bartel. Predicting effective microrna target sites in mammalian mrnas. *eLife*, 4:e05005, 2015.

[50] Gabriel F Berriz, Oliver D King, Barbara Bryant, Chris Sander, and Frederick P Roth. Characterizing gene sets with funcassociate. *Bioinformatics*, 19(18):2502–2504, 2003.

[51] Michael Ashburner, Catherine A Ball, Judith A Blake, David Botstein, Heather Butler, J Michael Cherry, Allan P Davis, Kara Dolinski, Selina S Dwight, Janan T Eppig, et al. Gene ontology: tool for the unification of biology. *Nature genetics*, 25(1):25–29, 2000.

[52] Antonia P Popova, J Kelley Bentley, Tracy X Cui, Michelle N Richardson, Marisa J Linn, Jing Lei, Qiang Chen, Adam M Goldsmith, Gloria S Pryhuber, and Marc B Hershenson. Reduced platelet-derived growth factor receptor expression is a primary feature of human bronchopulmonary dysplasia. *American Journal of Physiology-Lung Cellular and Molecular Physiology*, 307(3):L231–L239, 2014.

[53] Zoltan G Turi, Shereif Rezkella, Colin A Campbell, and Robert A Kloner. Left main percutaneous transluminal coronary angioplasty with the autoperfusion catheter in an animal model. *Catheterization and cardiovascular diagnosis*, 21(1):45–50, 1990.

[54] Arwen L Hunter, Jingchun Zhang, Shirley C Chen, Xiaoning Si, Brian Wong, Daryoush Ekhterae, Honglin Luo, and David J Granville. Apoptosis repressor with caspase recruitment domain (arc) inhibits myogenic differentiation. *FEBS letters*, 581(5):879–884, 2007.

[55] L Gortner, J Shen, and E Tutdibi. Sexual dimorphism of neonatal lung development. *Klinische Padiatrie*, 225(2):64–69, 2013.

[56] O Carvalho and C Goncalves. Expression of oestrogen receptors in foetal lung tissue of mice. *Anatomia, histologia, embryologia*, 41(1):1–6, 2012.

[57] Monique Brissett, Kristen L Veraldi, Joseph M Pilewski, Thomas A Medsger, and Carol A Feghali-Bostwick. Localized expression of tenascin in systemic sclerosis–associated pulmonary fibrosis and its regulation by insulin-like growth factor binding protein 3. *Arthritis & Rheumatism*, 64(1):272–280, 2012.

[58] Bing Xu, Cheng Chen, Hui Chen, Song-Guo Zheng, Pablo Bringas, Min Xu, Xianghong Zhou, Di Chen, Lieve Umans, An Zwijsen, et al. Smad1 and its target gene wif1 coordinate bmp and wnt signaling activities to regulate fetal lung development. *Development*, 138(5):925–935, 2011.

[59] Naho Fujiwara, Takashi Doi, Jan-Hendrik Gosemann, Balazs Kutasy, Florian Friedmacher, and Prem Puri. Smad1 and wif1 genes are downregulated during saccular stage of lung development in the nitrofen rat model. *Pediatric surgery international*, 28(2):189–193, 2012.

[60] Michael A Thompson and Richard M Weinshilboum. Rabbit lung indolethylamine n-methyltransferase cdna and gene cloning and characterization. *Journal of Biological Chemistry*, 273(51):34502–34510, 1998.

[61] Eugene P Kopantzev, Galina S Monastyrskaya, Tatyana V Vinogradova, Marina V Zinovyeva, Marya B Kostina, Olga B Filyukova, Alexander G Tonevitsky, Gennady T Sukhikh, and Eugene D Sverdlov. Differences in gene expression levels between early and later stages of human lung development are opposite to those between normal lung tissue and non-small lung cell carcinoma. *Lung Cancer*, 62(1):23–34, 2008.

[62] Norihiko Ohbayashi, Masamitsu Hoshikawa, Sachie Kimura, Masahiro Yamasaki, Shigeyuki Fukui, and Nobuyuki Itoh. Structure and expression of the mrna encoding a novel fibroblast growth factor, fgf-18. *Journal of Biological Chemistry*, 273(29):18161–18164, 1998.

[63] Michael Weinstein, XIAOLING Xu, Kyoji Ohyama, and Chu-Xia Deng. Fgfr-3 and fgfr-4 function cooperatively to direct alveogenesis in the murine lung. *Development*, 125(18):3615–3623, 1998.

[64] Mickey CT Hu, You-ping Wang, and Wan R Qiu. Human fibroblast growth factor-18 stimulates fibroblast cell proliferation and is mapped to chromosome 14p11. *Oncogene*, 18(16):2635–2642, 1999.

Figures and Tables

Figure 1:The *TPS* method. Given a dense sampling of a selected subset of genes (a) we select an initial set of points (b) using the initialization method described in the text. Next, we fit a spline to the selected points for each gene (c) and evaluate the error on all other points. We perform a greedy search process (d) which iteratively removes and adds points to improve the test data fit resulting in the final set of points (e). The reconstructed curves are fitted to all genes (f) and an overall error is computed and compared to the theoretical limit (noise) to determine the ability of the selected number of points to fit the data.

Figure 2: Performance of *TPS* using different sizes for the selected points.. Error comparisons of *TPS* variants to uniform selection of points and noise. Absolute difference - Greedy iterative addition with absolute difference initialization (Algorithm 1, Supporting Methods). Simulated annealing - Iterating using simulated annealing with absolute difference initialization. Weighted error - Selection based on cluster rather than individual gene errors. See Appendix Methods for details

Figure 3: Reconstructed expression profiles for selected genes. a) *Pdgfra*, b) *Eln*, c) *Inmt*

Figure 4: Performance of *TPS* by on the miRNA data. a) TPS reconstruction error when using the mRNA data to select time points for the miRNA experiments. Results of random and uniform selection as well as repeat noise error are also presented for comparison. TPS variants shown are the same two presented in Figure 2. b) Error of splines with points selected by training TPS on the actual miRNA data itself, using the maximum absolute difference initialization.

Figure 5: Comparison of gene expression and methylation data for selected genes. a) *Akt1*, b) *Cdh11*, c) *Tnc*.

Figure 6: Comparison of *TPS* with sampling rates used in previous studies. Dark green curves are the reconstructed profiles based on the points profiled by prior studies. Light green and red curves are based on the 5 and 8 points selected by *TPS*. As can be seen, even when comparing results from using the same number of points, *TPS* can identify key events for some of the genes that are missed when using the phenotype based sampling rates. Subfigures a,b, and c are a piecewise linear t over points 0.5,

7.0, 14.0, 28.0 . Subfigures d,e, and f are a piecewise linear fit over points 0.5, 2.0, 14.0, 28.0. Subfigures g,h, and i are a piecewise linear fit over points 0.5, 4.0, 7.0, 14.0, 28.0.

Figure 1 figure supplement 1: Comparison of performance between TPS and a previous method Singh et al. [13] which used an active learning method based on dynamic programming.

Figure 1 - figure supplement 2 : Comparison of initialization methods to each other by their final error. The points labeled metricA, metricB, and metricC all use the dynamic initialization approaches, while the max distance points use static initialization

Figure 1 - figure supplement 3 : Comparison of Initialization Method By their Final Error Compared to Selecting Random Points

Figure 2 - figure supplement 1: Average noise in each mRNA expression time point

Figure 2 - figure supplement 2: Comparison of TPS and piecewise linear fitting over genes a) *Pdgfra*, b)*Eln*, c) *Lrat*

Figure 2 - figure supplement 3 :Comparison of Error for the TPS algorithm on Full Data, 75% random Data, and Random Points Chosen on the Full Data. The 75% random data was created by replacing 75% of the gene time series with random value time series selected from a Gaussian distribution with mean 0 and standard deviation equal to the noise of the original data.

Figure 2 - figure supplement 4: Comparison of the reconstruction error when using the points selected by *TPS* and when using the same number of random points from the overall set of sampled points.

Figure 3 - figure supplement 1 : Expression profiles over several genes a) *Esr2*, b) *Nme3*, c) *Polr2a*

Figure 3 - figure supplement 2: Reconstructed expression proles by 8 points over genes a) *Pdgfra*, b) *Eln*, c) *Inmt*

Figure 4 - figure supplement 1: 8 stable miRNA clusters

Figure 4 - figure supplement 2: Observed and reconstructed expression proles for miRNAs a) *mmu-miR-100*, b) *mmu-miR-136*,c) *mmu-miR-152*, d) *mmu-miR-219*

Figure 4 - figure supplement 3 : TPS performance for the proteomics data using different number of time points.
a) Comparison of the reconstruction error when using the points selected by TPS, uniform selection of points, and when using the same number of random points from the overall set of sampled points.
b) Error comparisons of TPS to noise, and various search and initialization options discussed in Methods.

Figure 5 - figure supplement 1: Reconstructed methylation proles over several loci (chromosome, position) with corresponding genes.

Figure 5 - figure supplement 2 : Bootstrap analysis of Pearson correlation r between expression and methylation datasets over 8 time points for each gene. The red circles are the Pearson correlation over all 8 points and the blue triangles are the Pearson correlation for all subsets of 7 points.

Figure 6 - figure supplement 1 : Comparison of gene expression and protein abundance for selected gene protein pairs. a) *Eln / P54320*, b) *F13a1 / Q8BH61*, c) *Chil1 / Q61362*.

Supplementary File 1 : Raw mRNA expression values for the 126 genes studied using nanostring

Supplementary File 2 : Raw miRNA expression values from the nanostring analysis

Table 1: Summary of prior high throughput lung development studies

Reference	Data types	Selected time points (Days)
[37]	mRNA expression	E9, E4, E17, 0 ,7, 14, 28
[38]	mRNA expression	E16, E18, 0, 7, 14, 28
[39]	microRNA expression	E16, E19, E21, 0, 6, 14, 60
[40]	mRNA and microRNA expression	E12, E14, E16, 0, 2, 10
[20]	Protein expression levels	E12, E14, E18, 2, 14, 56
[6]	mRNA and miRNA expression	0, 4, 7, 14, 42
[41]	mRNA expression	0, 7, 14, adult
[42]	mRNA expression	E15, E17, E19, E21, 1, 14, 84
[43]	mRNA expression	E18, 1, 4, 7, 10, 14, 21, adult

1 Appendix Methods

1.1 Selecting the set of 126 genes

Table 1 provides the list of genes used for the nanostring analysis and the rational for their inclusion.

1.2 DNA Methylation analysis

Mouse alveolar lung tissues attached to LCM caps were stored at -80oC until processing. DNA was extracted using the ZR Genomic DNA-Tissue MicroPrep kit (Zymo Research). Incubation with Digestion buffer and proteinase K was done overnight at 55C in inverted tubes. 13 genes were chosen for targeted NextGen bisulfite sequencing (NGBS): *Igfbp3, Wif1, Cdh11, Eln, Sox9, Tnc, Dnmt3a, Akt, VEGF, Lox, FoxF2, ZFP536* and *Src*, based on published data [28]. The presence of CpG islands in 5-UTR, gene body and 3-UTR was interrogated using NCBI Epigenomics database, as well as CpG island searcher [44], and EMBOSS Cpgplot [45]. Targeted NGBS was done by Epigendx Inc. Gene sequences from selected regions were acquired from the Ensembl database. Gene IDs, transcript IDs, simplex PCR IDs, and target regions for each gene are listed in Appendix Table 3. A total of 42 target PCRs were designed by PyroMark Assay Design Software (Qiagen).

Targeted NGBS was done on samples collected at the following time points: E16.5, E18.5, P0.5, P1.5, P2.5, P5, P10, P15, P19 and P26. Mouse genomic DNA (200-500 ng) was bisulfite treated using the EZ DNA Methylation Kit (Zymo Research). Multiplex PCR was performed using 0.5 units of TaKaRa EpiTaq HS (Takara Bio) in 2x master mix.

FASTQ files were aligned using open source Bismark Bisulfite Read Mapper using Bowtie2. Methylation levels were calculated in Bismark by dividing the number of methylated reads by the number of total reads, considering all CpG sites covered by a minimum of 30 total reads. Sites where the difference in methylation was less than 5% over the entire time period, those where there was a difference of $> 20\%$ at a single time point and those with less than 3 non zero values were removed from the analyses.

1.3 *TPS* Algorithm

A pseudocode for the *TPS* algorithm is presented in Algorithm 1.

1.4 Selecting the initial set of points

When using an iterative algorithm to solve non-convex problems with several local minima, a key issue is the appropriate selection of the initial solution set. We have tested a number of methods for performing such initializations. The simplest method we tried is to uniformly select a subset of the points (so if $k = T/4$ we use each 4'th point). Another method we tested is to partition the set of all time points T into $k-1$ intervals of almost equal size. This method determines these boundaries by estimating the cumulative number of points until each time point and selecting time points

Algorithm 1 *TPS*: Iterative k-point selection

procedure ITERATIVE–TEMPORAL–SELECTION
  C_0 = select initial k time points by absolute difference sorting
  e_0 = error of remaining points by fitting splines to C_0
  $i = 0$
  do
    for each pair $(t_a, t_b) \in (T^- \setminus C_i) \times C_i$ **do**
      $C^* = C_i \cup \{t_a\} \setminus \{t_b\}$
      e^* = estimate error by fitting smoothing spline to C^* where regularization parameter is estimated by LOOCV
      if $e^* < e_i$ **then**
        $C_{i+1} = C^*$
        $e_{i+1} = e^*$
      end if
      $i = i + 1$
    end for
  while $e_{i+1} < e_i$
  Output C_i and e_i
end procedure

with cumulative values $\frac{T}{k-1}, 2\frac{T}{k-1}, \ldots, (k-2)\frac{T}{k-1}$ respectively. Then, it uses k interval boundaries including t_1 and t_T as initial solution. We also tested a method that relies on the changes between consecutive time points to select the most important ones for our initial set. Specifically, we sort all points except t_1 and t_T by average absolute difference with respect to its predecessor and successor time points by computing:

$$m_{t_i} = \frac{\sum_{g \in G} |Md(e_{gt_{i-1}}) - Md(e_{gt_i})| + |Md(e_{gt_{i+1}}) - Md(e_{gt_i})|}{2|G|} \tag{2}$$

where $Md(e_{gt_i})$ is the median expression for gene g at time t_i. We then select the $k-2$ points with maximum m_{t_i} as the initial solution.

Finally, we developed an alternative initialization method, based on dyanmic recalculation of a metric on each time point. Metric A is same equal to the equation shown above. Metric B of a time point is the difference absolute difference with respect to its predecessor and successor time points. Metric C of a time point is absolute difference with respect to only its predecessor. The alternative initialization algorithm calculates the given metric on each time point other than the first and last and then places those points in a min heap based on the metric. The top(minimum) point in the heap is removed. The metric is recalculated for the point's predeccesor and succesor based on thier neighboring points, using only the points remaining in the heap. This process is repated until only k-2 time points remain in the heap. Then the first time point, last time point and the points remaind in the heap are chosen.

$$MetricA_{e,t_i} = \frac{\sum_{g \in G} |(Md(e_{gprevious_{t_i}}) - Md(e_{gt_i})) + (Md(e_{gnext_{t_i}}) - Md(e_{gt_i}))|}{2|G|} \quad (3)$$

$$MetricB_{e,t_i} = \frac{\sum_{g \in G} |(Md(e_{gprevious_{t_i}}) - Md(e_{gt_i})) - (Md(e_{gnext_{t_i}}) - Md(e_{gt_i}))|}{2|G|} \quad (4)$$

$$MetricC_{e,t_i} = \frac{\sum_{g \in G} |(Md(e_{gprevious_{t_i}}) - Md(e_{gt_i}))}{2|G|} \quad (5)$$

Algorithm 2 Init TPS: Iterative initial k point selection

procedure ITERATIVE–INITIAL POINT–SELECTION
H = Empty min heap
e = matrix where rows are genes and columns are time points, values are expression measurements
for each time point t (other than the first and last) **do**
$value_t = Metric_{e,t}$
$previous_t = t - 1$
$next_t = t + 1$
Add $value_t$ to H
end for
while $size(H) > k - 2$ **do**
Remove minimum $value_m$ time point m from H
$previous_{next_m} = previous_m$
$next_{previous_m} = next_m$
Remove $value_{previous_m}$ from H
Remove $value_{next_m}$ from H
Remove m from e
$value_{previous_m} = Metric_{e,previous_m}$
$value_{next_m} = Metric_{e,next_m}$
Add $value_{next_m} toH$
Add $value_{previous_m} toH$
end while
Ouput all t left as $value_t$ in H + first time point + last time point
end procedure

We found that for our particular dataset, the dynamic initialization with $MetricA_{e,t_i}$ performed best for selections of time points smaller than one third of the the initial dense time series, while the non dynamic m_{t_i} method works best for selections of time points between one third and and one half of the initial time series. The dyanmic metric and non dynamic metrics can be compared in their performance on our data in Figure 1 - figure supplement 2. However, all of the metrics performed much better than a selection of random points as shown in Figure 1 - figure supplement 3.

1.5 Further Improvements to the Iterative Points Selection Procedures

We tested the following possible search strategies to improve the iterative points removal and addition in *TPS*.

- We add and remove b time points in each iteration instead of a single point. This increases the complexity of each iteration from $O(kGT^2Q)$ to $O(kGT^{2b}Q)$ where Q is the complexity of fitting a smoothing spline.
- We use simulated annealing to escape from local minima [46]. In this case, we do not always move to a pair of points with the minimum error in each iteration, but instead move to a solution with random pair of points with probability 1 if its error e^r is lower than error of current solution e^i whereas we move to a solution with probability $e^{-C(e^r-e^i)}$ if $e^r \geq e^i$. Here, C is the temperature that increases by increasing number of iterations and the probability of moving to a solution with larger error decreases over time.

In practice, even though both approaches should in theory be better able to escape local minima than the greedy approach described above, for the data we analyzed they do not perform significantly better as Figure 2 in the main text demonstrates.

1.6 Fitting Smoothing Spline

TPS uses splines for fitting expression curves. Regularized smoothing spline satisfies the piecewise cubic polynomial $\mu(t) = a_i + b_i(t-t_i) + c_i(t-t_i)^2 + d_i(t-t_i)^3$ for $t \in [t_i, t_{i+1})$, $i \in 1, \ldots, T-1$ as shown in [30]. Then, according to [29, 47], regularized smoothing spline objective can also be expressed as in:

$$\min (y-a)^{'}(y-a) + \lambda c^{'} R c \tag{6}$$

where $a = (a_1, a_2, \ldots, a_T)$, $c = (c_2, c_3, \ldots, c_{T-1})$, and R is a $(n-2)^2$ tridiagonal symmetric matrix with entries $r_{i,i} = \frac{2(h_i+h_{i+1})}{3}$, $r_{i,i+1} = \frac{h_{i+1}}{3}$ where $h_i = t_{i+1} - t_i$. The continuity restrictions imply that:

$$Rc = Q^{'} a \tag{7}$$

where Q is an $n \times (n-2)$ tridiagonal matrix with entries $q_{i,i+1} = \frac{1}{h_{i+1}}$, $q_{i+1,i} = \frac{1}{h_{i+1}}$ and $q_{i,i} = -(\frac{1}{h_i} + \frac{1}{h_{i+1}})$. Thus, we may write Eq. 6 as:

$$\min (y-a)^{'}(y-a) + \lambda a^{'} Q R^{-1} Q^{'} a \tag{8}$$

where a can be derived as in:

$$a = (I + \lambda Q R^{-1} Q^{'})^{-1} y \tag{9}$$

Once a is estimated, b, c, d are estimated by corresponding Equations in [47].

For our specific setting, we also introduce a regularization parameter to enable us to determine the number of control points. Let $I_g = \{(t, Md(e_{gt})),\ t \in C\}$, and μ be the spline we are interested in fitting, smoothing spline can be found by the following optimization problem which minimizes penalized least-squares error:

$$\min \sum_{(t,y_t)\in I_g} (y_t - \mu(t))^2 + \lambda \int_{t_1}^{t_T} \mu''(x)^2 dx \tag{10}$$

where λ is the regularization parameter which prevents overfitting by affecting the number of knots selected. We estimated λ by leave-one-out cross-validation (LOOCV) in our experiments (See Appendix Methods for details of smoothing spline fitting).

1.7 Proteomics analysis

Proteins were extracted using tissue protein extraction reagent (T-PER, Thermo) as per manufacturers instructions, carried out directly on the micro-dissection cap. Protein concentrations was determined with the EZQ protein assay (Life Sciences). The proteins were digested overnight at 37C, followed by acidification to pH $3-4$ with 10% formic acid (FA), and extracted as per manufacturers instructions, then concentrated to near completion using a Savant SpeedVac Concentrator (Thermo) and diluted with 0.1% FA to a final concentration of $\sim$ 100ng \uL for analysis by LCMS. The LCMS data were converted to a universal MzXML file format prior to being searched using SEQEST (Thermo) against a Mouse subset of the UniRef100 database. These data were then uploaded to Scaffold (Proteome Software) in order to filter and group each peptide ID to specific proteins with peptide probability scores set at 80%, and protein probability scores set at 99%. Using only proteins presenting with 2 or more peptides per protein, the confidence interval was set to $\sim$ 99.9% with and FDR < 0.1. Quantification was carried out using Scaffold Q + using normalized spectral counts.

2 Appendix Results

2.1 Example of a *TPS* run

Here we discuss a specific setting for *TPS* that allows us to discuss the set of points selected and their relevance. Specifically, to test *TPS*, we fixed three set points in advance (first (0.5'th day) and last (28'th day), which are required for any setting and day 7 which was previously determined to be of importance to lung development. Next, we have asked *TPS* to further select 10 more points (for a total of 13). For this setting, the method selected the following points: 0.5, 1.0, 1.5, 2.5, 4, 5, 7, 10, 13.5, 15, 19, 23, 28. While we do not know the ground truth, the larger focus on the earlier time points determined by the method (with 7 of the 13 points for the first 7 days) makes sense in this context as several aspects of lung differentiation are determined in the first week [48].

The other 3 weeks were more or less uniformly sampled by our *TPS*. This highlights the usefulness of an unbiased approach to sampling time points rather than just uniformly sampling through the time window.

2.2 *TPS* identifies subset of important time points across multiple genes

To understand whether gene-expression profiles over time has a simple trend, we also compare the reconstruction performance of *TPS* with fitting piecewise linear curves between initial and middle time points and between middle and last time points. The reconstruction error by *TPS* is significantly better than the piecewise linear reconstruction for 102 genes out of 126 genes. We have plotted the comparison of reconstruction for several of these genes as in Figure 2 - figure supplement 2. The distribution of error difference between these methods looks significantly different than normal distribution ($p < 0.0001$ by Shapiro-Wilk test).

2.3 miRNA Clusters Are Enriched For Several Biological Processes

While the mRNA datasets includes only a handful of genes (less than 0.5% of all genes) the miRNA data includes more profiles and so further analysis of this data can be perfromed. We have performed clustering of the miRNA data using k-means [33] where the number of clusters is selected by Bayesian Information Criteria [36] leading to 8 stable miRNA clusters Figure 4 - figure supplement 1. Next, we mapped miRNA's to predicted targets using TargetScan [49], and performed gene-enrichment analysis by FuncAssociate [50]. We find clusters to be enriched for several Gene Ontology biological processes [51]. For instance, cluster 4 is enriched for single-organism cellular process, positive regulation of biological process, regulation of metabolic process, etc. See Supporting Website for complete results.

2.4 miRNA Reconstruction

Figure 4 - figure supplement 2 presents the reconstructed and measured expression values for a few miRNAs based on time points identified using the mRNA dataset. Several of these miRNAs are known to be involved in regulation of lung development. For example, *mmu-miR-100* is known to regulate *Fgfr3* and *Igf1r*, *mmu-miR-136* targets *Tgfb2*, *mmu-miR-152* targets *Meox2, Robo1, Fbn1, Nfya* [52]. Additional figures for all miRNAs and mRNAs are avialable on the supporting website.

2.5 *TPS* application to select time points for proteomics analysis

We used mass spectrometry to profile the levels of 1020 proteins over the optimal 13 time points determined by *TPS* (using the mRNA expression data): $[0.5, 1.0, 1.5, 2.5, 4.0, 5.0, 7.0, 10.0, 13.5, 15.0, 19.0, 23.0, 28.0]$). To test the ability of *TPS* to determine the optimal time points for the proeomics data (based only on the mRNA data) we performed a similar analysis to the analysis performed for the miRNA

data. Specifically, we used *TPS* to select subset of 4 to 12 of these points *based on the mRNA data* and compared the error using these points to random and uniform selection of the same number of points. The results are presented in . In addition to comparing *TPS* to random and uniform we have also compared different strategies for initializing the set of points as discussed in Method. Finally, the figure also presents the repeat noise values which is the theoretical limit for the performance of any profile reconstruction method.

As for the miRNA data, we see a significant and consistent improvement (for all number of selected time points) over uniform sampling highlighting the advantage of condition specific sampling decisions. Again, as the number of points used by *TPS* increases, it leads to results that are very close to the error represented by noise in the data (17.47).

2.6 Analysis of Methylation Data

Methylation data included 3 repeats for time points 0.5, 1.5, 2.5, 5, 10, 15, 19, 26 for 266 loci belonging to 13 genes. Among these genes all except *Zfp536* were also profiled in our nanostring mRNA analysis. Appendix Table 2 summarizes the number of loci for each gene in the methylation dataset. We used shifted percentage of methylation at each time point in our analysis which is obtained by subtracting the median percentage of methylation at initial time point (baseline) from all data points for each gene. Figure 5 - figure supplement 2 presents the best positive or negative correaltion observed between the methylation data and the gene expression data for these genes (note that we do not expect all up stream regions to show a correlated profile since it is likely that only a subset, or even a single, region is responsible for the changes in expression observed which is why we look for the most correlated or anti-correlated region).

2.7 Importance of correct determination of expression profiles

As shown in Figure 6 in the main text, *TPS* results differ from prior methods when reconstructing expression profiles for several genes. Below we discuss the significance of these differences and their impact on the ability to correctly assign function to that gene:

- *Nol3*: Nucleolar protein 3 (apotosis repressor with CAR domain) gene (also called *ARC*) encodes a protein that inhibits apoptosis, by decreasing activities of Caspases 2 and 8 and tumor protein p53. Evaluation of the *TPS* profile suggests that the increase in Nol3 correlates with postnatal lung development, with a rapid increase from birth until 2 weeks of age, followed by stabilization, while the prior sampling rates show only an initial peak and then decrease. While the exact role of *Nol3* in lung development has not been established, it is known that *Nol3* protects pulmonary arterial smooth muscle cells from hypoxia-induced death and facilitates growth factor-induced proliferation and hypertrophy, and is probably involved in human pulmonary hypertension [53]. *Nol3* is a regulator of myogenic differentiation [54]

and its pattern of expression suggests that it may be important in regulating pulmonary airway and vascular smooth muscle development and differentiation.

- *Esr2*: The gene estrogen receptor beta encodes a receptor for estrogen, and is important in regulating lung development and modulating differences in lung development between males and females [55]. Evaluation of the *TPS* profile suggests that the *Esr2* decreases briefly after birth, followed by an increase from around day 5 until day 20 whereas non-optimized profile suggests a relatively flat profile. While fetal mouse lungs express both *Esr2* alpha and beta, adult mouse lungs express only *Esr2* beta consistent with the TPS results [56].

- *Igfbp3*: Insulin-like growth factor binding protein 3 (*Igfbp3*) belongs to the Igfbp family and has a Igfbp domain and a thyroglobulin type-I domain (`http://www.ncbi.nlm.nih.gov/gene/3486`). The *TPS* profile for *Igfbp3* is very different from the non-optimized profile, suggesting that important biological information is lost when not using the *TPS* profile. *Igfbp3* regulates the induction of TNC by TGF-beta [57] and both these molecules are critical in lung alveolar septation.

- *Wif1*: *Wnt* inhibitory factor 1 (*WIF1*) inhibits Wnt proteins, that are well known to be critical in many stages of lung development. The *TPS* profile is very different from the non-optimized profile, as the *TPS* profile indicates a much earlier and higher peak of *WIF1* during postnatal lung development that may be critical in alveolar septation. *WIF1* is a target gene for Smad1, one of the *BMP* receptor proteins important in lung development and maturation. A regulatory loop of *Bmp4-Smad1-Wif1-Wnt/beta-catenin* may coordinate *BMP* and *Wnt* pathways to control lung development [58], and dysregulation of the *Smad1/Wif1* axis is associated with lung hypoplasia [59].

- *Inmt*: Indolethylamine N-methyl transferase (*Inmt*) gene encodes an enzyme that N-methylates indoles such as tryptamine (`http://www.ncbi.nlm.nih.gov/gene/11185`). The TPS profile for *Inmt* is very different from the non-optimized profile, as the *TPS* profile indicates a much lower and prolonged reduction of *Inmt* during postnatal lung development. Methyl conjugation is an important pathway in the metabolism of many drugs, neurotransmitters, and xenobiotic compounds [60]. While it is known that *Inmt* expression varies over the course of human lung development [61], its exact role in lung development is not known.

- *Fgf18*: Fibroblast growth factor 18 (*Fgf18*) is a member of the fibroblast growth factor family, and the Fgfs are well known to be critical in multiple stages of lung development. The non-optimized profile indicates a smaller and later peak, and is not similar to the *TPS* profile which suggests a much more improtant role.*Fgf18* is a pleiotropic growth factor that stimulates proliferation in a number of tissues (`http://www.ncbi.nlm.nih.gov/gene/8817`).

Fgf18 is highly expressed in the developing lung as the *TPS* profile indicates [62], and Fgfr3 is important in postnatal alveolar development [63]. The role of *Fgf18* in regulating fibroblast proliferation [64] may be important in alveolar septation, as *Fgf18* increases after birth with a peak around P10, with reduction after completion of alveolar septation.

Appendix Tables

Ensembl Gene ID	Accession number	*gene name*	Rationale
ENSMUSG00000024130	NM_001039581.2	*Abca3*	Alveolar Type II cell marker
ENSMUSG00000031378	NM_007435.1	*Abcd1*	important in other processes (IPF, COPD etc)
ENSMUSG00000029802	NM_011920.3	*Abcg2*	Mesenchymal cell marker
ENSMUSG00000035783	NM_007392.3	*Acta2*	Fibroblast cell marker
ENSMUSG00000029580	NM_007393.1	*Actb*	Common house-keeping gene
ENSMUSG00000036040	NM_029981.1	*Adamtsl2*	Altered DNA methylation during septation
ENSMUSG00000015452	NM_007425.2	*Ager*	Alveolar Type I cell marker
ENSMUSG00000001729	NM_001165894.1	*Akt1*	Altered DNA methylation during septation
ENSMUSG00000053279	NM_013467.3	*Aldh1a1*	Important for septation
ENSMUSG00000013584	NM_009022.3	*Aldh1a2*	Potentially important for septation
ENSMUSG00000022244	NM_008537.4	*Amacr*	important in other processes (IPF , COPD etc)
ENSMUSG00000044217	NM_009701.4	*Aqp5*	Alveolar Type I cell marker
ENSMUSG00000026576	NM_009721.5	*Atp1b1*	Lung fluid clearance
ENSMUSG00000060802	NM_009735.3	*B2m*	Common house-keeping gene
ENSMUSG00000102037	NM_009742.3	*Bcl2a1a*	Apoptosis regulator
ENSMUSG00000056216	NM_009884.3	*Cebpg*	Important for lung development
ENSMUSG00000029084	NM_007646.4	*Cd38*	Airway smooth muscle cell functional responses
ENSMUSG00000018774	NM_009853.1	*Cd68*	Monocyte cell marker
ENSMUSG00000031673	NM_009866.4	*Cdh1*	Epithelial cell marker
ENSMUSG00000064246	NM_007695.2	*Chil1*	Monocyte cell marker
ENSMUSG00000040809	NM_009892.1	*Chil3*	Increased during septation
ENSMUSG00000022512	NM_016674.3	*Cldn1*	Tight junction protein
ENSMUSG00000070473	NM_009902.4	*Cldn3*	Tight junction protein (mostly epithelial)
ENSMUSG00000041378	NM_013805.4	*Cldn5*	Tight junction protein
ENSMUSG00000018569	NM_016887.6	*Cldn7*	Tight junction protein (mostly epithelial)
ENSMUSG00000001506	NM_007742.3	*Col1a1*	Fibroblast cell marker
ENSMUSG00000063063	NM_009819.2	*Ctnna2*	Altered DNA methylation during septation
ENSMUSG00000031360	NM_001168571.1	*Ctps2*	important in other processes (IPF , COPD etc)
ENSMUSG00000040856	NM_010052.4	*Dlk1*	Decreased during septation
ENSMUSG00000020661	NM_007872.4	*Dnmt3a*	Altered DNA methylation during septation
ENSMUSG00000046179	NM_001013368.5	*E2f8*	Altered DNA methylation during septation
ENSMUSG00000000303	NM_009864.2	*Cdh1*	Epithelial cell marker
ENSMUSG00000020122	NM_207655.2	*Egfr*	Important for lung development
ENSMUSG00000029675	NM_007925.3	*Eln*	Altered DNA methylation during septation
ENSMUSG00000045394	NM_008532.2	*Epcam*	Epithelial cell marker
ENSMUSG00000052504	NM_010140.3	*Epha3*	Involved in lung development
ENSMUSG00000028289	NM_001122889.1	*Epha7*	Involved in lung cancer, potential role in development
ENSMUSG00000021055	NM_010157.3	*Esr2*	Important regulator of multiple processes
ENSMUSG00000061731	NM_010162.2	*Ext1*	Altered DNA methylation during septation
ENSMUSG00000039109	NM_001166391.1	*F13a1*	Involved in lung injury , cancer
ENSMUSG00000057967	NM_008005.1	*Fgf18*	Important for septation
ENSMUSG00000030849	NM_010207.2	*Fgfr2*	Important regulator of multiple processes
ENSMUSG00000078302	NM_008242.2	*Foxd1*	Pericyte cell marker
ENSMUSG00000042812	NM_010426.1	*Foxf1*	Involved in lung development
ENSMUSG00000038402	NM_010225.1	*Foxf2*	Altered DNA methylation during fibrosis
ENSMUSG00000001020	NM_011311.1	*S100a4*	Fibroblast cell marker
ENSMUSG00000057666	NM_001001303.1	*Gapdh*	Common house-keeping gene
ENSMUSG00000005836	NM_010258.3	*Gata6*	Important regulator of multiple processes
ENSMUSG00000029992	NM_013528.3	*Gfpt1*	important in other processes (IPF, COPD etc)
ENSMUSG00000041624	NM_001033322.2	*Gucy1a2*	Important for septation
ENSMUSG00000025534	NM_010368.1	*Gusb*	Common house-keeping gene
ENSMUSG00000021109	NM_010431.2	*Hif1a*	Hypoxia signaling
ENSMUSG00000058773	NM_020034.1	*Hist1h1b*	Decreased during septation
ENSMUSG00000061615	NM_175660.3	*Hist1h2ab*	Decreased during septation
ENSMUSG00000032126	NM_013551.2	*Hmbs*	Common house-keeping gene
ENSMUSG00000029919	NM_019455.4	*Hpgds*	important in other processes (IPF, COPD etc)
ENSMUSG00000025630	NM_013556.2	*Hprt*	Common house-keeping gene
ENSMUSG00000020053	NM_001111274.1	*Igf1*	Regulating miRNA altered during septation
ENSMUSG00000020427	NM_008343.2	*Igfbp3*	Altered DNA methylation during septation, fibrosis
ENSMUSG00000003477	NM_009349.3	*Inmt*	Increased during septation
ENSMUSG00000026768	NM_001001309.2	*Itga8*	Involved in lung development

ENSMUSG00000040029	NM_001081113.1	*Ipo8*	important in other processes (IPF, COPD etc)
ENSMUSG00000030786	NM_001082960.1	*Itgam*	Monocyte cell marker
ENSMUSG00000030789	NM_021334.2	*Itgax*	Monocyte cell marker
ENSMUSG00000090122	NM_021487.1	*Kcne1l*	important in other processes (IPF, COPD etc)
ENSMUSG00000063142.10	XM_006518608.1	*Kcnma1*	Altered DNA methylation during septation
ENSMUSG00000079852	NM_010649.3	*Klra4*	Increased during septation
ENSMUSG00000023043	NM_010664.2	*Krt18*	Epithelial cell marker
ENSMUSG00000061527	NM_027011.2	*Krt5*	Basal cell marker
ENSMUSG00000029570	NM_008494.3	*Lfng*	Important for septation
ENSMUSG00000024529	NM_010728.2	*Lox*	Altered DNA methylation during fibrosis
ENSMUSG00000028003	NM_023624.4	*Lrat*	Increased during septation
ENSMUSG00000027070	NM_001081088.1	*Lrp2*	Altered DNA methylation during septation
ENSMUSG00000061068	NM_010779.2	*Mcpt4*	Decreased during septation
ENSMUSG00000026110	NM_173870.2	*Mgat4a*	Involved in acute lung injury
ENSMUSG00000043613	NM_010809.1	*Mmp3*	Increased during septation
ENSMUSG00000018623	NM_010810.4	*Mmp7*	Important in lung fibrosis
ENSMUSG00000066108	XM_006508653.1	*Muc5b*	Important in lung fibrosis
ENSMUSG00000037974	NM_010844.1	*Muc5ac*	Epithelial cell marker
ENSMUSG00000024304	NM_007664.4	*Cdh2*	Tight Junction/Adhesion
ENSMUSG00000054008	NM_008306.4	*Ndst1*	Involved in pathologic airway remodeling
ENSMUSG00000031902	NM_010901.2	*Nfatc3*	Important for lung development
ENSMUSG00000073435	NM_019730.2	*Nme3*	Apoptosis-related gene
ENSMUSG00000026575	NM_138314.3	*Nme7*	Important for stem cell renewal
ENSMUSG00000014776	NM_030152.4	*Nol3*	Regulating miRNA altered during septation
ENSMUSG00000051048	NM_177161.4	*P4ha3*	Important in lung fibrosis
ENSMUSG00000068039	NM_013686.3	*Tcp1*	Basal cell marker
ENSMUSG00000029998	NM_025823.4	*Pcyox1*	important in other processes (IPF , COPD etc)
ENSMUSG00000029231	NM_011058.2	*Pdgfra*	Important for septation
ENSMUSG00000024620	NM_008809.1	*Pdgfrb*	Pericyte cell marker
ENSMUSG00000028583	NM_010329.2	*Pdpn*	Alveolar Type I cell marker
ENSMUSG00000062070	NM_008828.2	*Pgk1*	important in other processes (IPF , COPD etc)
ENSMUSG00000053398	NM_016966.3	*Phgdh*	important in other processes (IPF, COPD etc)
ENSMUSG00000005198	NM_009089.2	*Polr2a*	important in other processes (IPF, COPD etc)
ENSMUSG00000071866	NM_008907.1	*Ppia*	Common house-keeping gene
ENSMUSG00000024997	NM_007452.2	*Prdx3*	Mitochondrial oxidative stress regulator
ENSMUSG00000026134	NM_008922.2	*Prim2*	Expressed in placenta and crucial for mammalian growth.
ENSMUSG00000033491	NM_178738.3	*Prss35*	Decreased during septation
ENSMUSG00000032487	NM_011198.3	*Ptgs2*	Regulating miRNA altered during septation
ENSMUSG00000056458	NM_011973.2	*Mok*	Alveolar Type I cell marker
ENSMUSG00000037992	NM_001177302.1	*Rara*	Important for septation
ENSMUSG00000022883	NM_019413.2	*Robo1*	Altered DNA methylation during septation
ENSMUSG00000025508	NM_026020.6	*Rplp2*	
ENSMUSG00000066361	NM_008458.2	*Serpina3c*	Increased during septation
ENSMUSG00000022097	NM_011359.1	*Sftpc*	Alveolar Type II cell marker
ENSMUSG00000021795	NM_009160.2	*Sftpd*	Alveolar Type II cell marker
ENSMUSG00000050010	NM_001033415.3	*Shisa3*	Altered DNA methylation during septation
ENSMUSG00000032402	NM_016769.3	*Smad3*	Important for septation
ENSMUSG00000042821	NM_011427.2	*Snai1*	Important for lung development and injury
ENSMUSG00000000567	NM_011448.4	*Sox9*	Altered DNA methylation during septation
ENSMUSG00000027646	NM_001025395.2	*Src*	Altered DNA methylation during septation
ENSMUSG00000014767	NM_013684.3	*Tbp*	Common house-keeping gene , involved in multiple processes
ENSMUSG00000000094	NM_172798.1	*Tbx4*	Altered DNA methylation during septation
ENSMUSG00000032228	NM_011544.3	*Tcf12*	Involved in multiple developmental processes
ENSMUSG00000022797	NM_011638.3	*Tfrc*	Common house-keeping gene
ENSMUSG00000002603	NM_011577.1	*Tgfb1*	Important for septation
ENSMUSG00000045691	NM_153083.5	*Thtpa*	important in other processes (IPF, COPD etc)
ENSMUSG00000032011	NM_009382.3	*Thy1*	Fibroblast cell marker
ENSMUSG00000028364	NM_011607.1	*Tnc*	Altered DNA methylation during septation
ENSMUSG00000044986	NM_009437.4	*Tst*	important in other processes (IPF, COPD etc)
ENSMUSG00000026803	NM_009442.2	*Ttf1*	Important for lung development
ENSMUSG00000008348	NM_019639.4	*Ubc*	Common house-keeping gene
ENSMUSG00000023951	NM_001025250.3	*Vegfa*	Angiogenesis; Altered DNA methylation during septation
ENSMUSG00000026728	NM_011701.4	*Vim*	Mesenchymal cell marker
ENSMUSG00000020218	NM_011915.1	*Wif1*	Altered DNA methylation during septation

ENSMUSG00000022285	NM_011740.2	*Ywhaz*	Common house-keeping gene

Appendix Table 1: List of genes used for the Nanostring analysis and the rational for their inclusion.

Gene	Number of loci		Gene	Number of loci
Cdh11	14		*Zfp536*	16
Src	11		*Igfbp3*	34
Sox9	16		*Wif1*	21
Dnmt3a	41		*Vegfa*	20
Eln	20		*Tnc*	4
Foxf2	41		*Lox*	17
Akt1	11			

Appendix Table 2: Summary of methylation dataset

Gene	Ensembl Gene ID	Ensembl Transcript ID	Assay ID	Target Location	Fwd Tm	Rev Tm	% GC	Coordinates (GRCm38/mm10)
Akt1	ENSMUSG00000001729	ENSMUST00000001780	ADS3333	3' UTR	68	65.5	31.5	chr12:112654548-112654709
Akt1	ENSMUSG00000001729	ENSMUST00000001780	ADS3332	Intron 9/Exon 10	68.3	69.8	38.3	chr12:112657120-112657273
Cdh11	ENSMUSG00000031673	ENSMUST00000075190	ADS3308	Intron 3	66.8	68.3	36.9	chr8:102677609-102677766
Cdh11	ENSMUSG00000031673	ENSMUST00000075190	ADS3318	Intron 1	64.1	69.7	37	chr8:102784569-102784722
Cdh11	ENSMUSG00000031673	ENSMUST00000075190	ADS3307	Promoter	69.1	71.3	29.9	chr8:102785456-102785649
Dnmt3a	ENSMUSG00000020661	ENSMUST00000020991	ADS3326	Promoter	68.6	67.7	47.1	chr12:3806505-3806659
Dnmt3a	ENSMUSG00000020661	ENSMUST00000020991	ADS632	Intron 1	64	64.7	32.2	chr12:3834382 -3834592
Dnmt3a	ENSMUSG00000020661	ENSMUST00000020991	ADS3328	Exon 6/Intron 6	64.7	64	31.8	chr12:3901545-3901764
Dnmt3a	ENSMUSG00000020661	ENSMUST00000020991	ADS3329	Intron 6	66.8	66.1	25.4	chr12:3907514-3907765
Eln	ENSMUSG00000029675	ENSMUST00000015138	ADS3319	Intron 16	67.1	67.9	47.8	chr5:134721191-134721447
Eln	ENSMUSG00000029675	ENSMUST00000015138	ADS3309	Intron 7/Exon 8/Intron 8	64.1	67.4	37.8	chr5:134729221-134729526
Eln	ENSMUSG00000029675	ENSMUST00000015138	ADS024	Promoter	65	67.4	42.6	chr5:134747412-134747606
Foxf2	ENSMUSG00000038402	ENSMUST00000042054	ADS4505	Promoter	63.1	65	42.5	chr13: 31625470-31625556
Foxf2	ENSMUSG00000038402	ENSMUST00000042054	ADS4506	5-UTR	65.1	64.8	37.9	chr13:31625904-31626093
Foxf2	ENSMUSG00000038402	ENSMUST00000042054	ADS4507	3-Downstream	68	68.9	28.1	chr13:31632481-31632716
Igfbp3	ENSMUSG00000020427	ENSMUST00000020702	ADS5134	3-Downstream	69.3	69.6	32.1	chr11:7203969-7204208
Igfbp3	ENSMUSG00000020427	ENSMUST00000020702	ADS3301	Exon 4/Intron 4	70.5	70	33	chr11:7208306-7208481
Igfbp3	ENSMUSG00000020427	ENSMUST00000020702	ADS5133	Intron 1	68.3	68.5	26.1	chr11:7212803-7213043
Igfbp3	ENSMUSG00000020427	ENSMUST00000020702	ADS5132	Promoter	67.8	69.2	28.7	chr11:7214210-7214499
Lox	ENSMUSG00000024529	ENSMUST00000171470	ADS4512	Exon 2	69	70.9	31.3	chr18: 52529184-52529315
Lox	ENSMUSG00000024529	ENSMUST00000171470	ADS4513	Exon 4	65.7	64.8	28.5	chr18:52526887-52527023
Lox	ENSMUSG00000024529	ENSMUST00000171470	ADS4511	Promoter	64.7	66.4	21.2	chr18:52530080-52530216
Sox9	ENSMUSG00000000567	ENSMUST00000000579	ADS796	Promoter	61	66.1	31.4	chr11:112781641-112781811
Sox9	ENSMUSG00000000567	ENSMUST00000000579	ADS3311	Intron 1	69.7	68.5	34.7	chr11:112783358-112783605
Sox9	ENSMUSG00000000567	ENSMUST00000000579	ADS3310	Exon 3	66.4	63.1	26.2	chr11:112784760-112784885
Src	ENSMUSG00000027646	ENSMUST00000109533	ADS4514	Intron 1	64.8	65.9	35.9	chr2:157423925-157424027
Src	ENSMUSG00000027646	ENSMUST00000109533	ADS4515	Intron 4	66.5	68.8	37.6	chr2:157457351-157457520
Src	ENSMUSG00000027646	ENSMUST00000109533	ADS4516	Exon 14	65.5	65.6	33.7	chr2:157469741-157469912
Tnc	ENSMUSG00000028364	ENSMUST00000107377	ADS3324	Intron 14	63.3	62.2	23	chr4:63982645-63982818
Tnc	ENSMUSG00000028364	ENSMUST00000107377	ADS3325	Intron 14	62.5	61.6	20.2	chr4:63982799-63982986
Tnc	ENSMUSG00000028364	ENSMUST00000107377	ADS3323	Exon 3	65	67.5	35.2	chr4:64017478-64017721
Tnc	ENSMUSG00000028364	ENSMUST00000107377	ADS3322	Promoter	62.7	63.9	26.7	chr4:64047034-64047149
Vegfa	ENSMUSG00000023951	ENSMUST00000071648	ADS3336	3-UTR	67.2	66.9	32.6	chr17:46018598-46018735
Vegfa	ENSMUSG00000023951	ENSMUST00000071648	ADS3335	Intron 2/Exon 3	64.6	63.8	29.5	chr17:46025336-46025620
Wif1	ENSMUSG00000020218	ENSMUST00000020439	ADS3302	Promoter	69.4	68.7	31.3	chr10:121033395-121033691
Wif1	ENSMUSG00000020218	ENSMUST00000020439	ADS3303	Intron 4/Exon 5/Intron 5	60.9	60.1	31.8	chr10:121083800-121083997
Wif1	ENSMUSG00000020218	ENSMUST00000020439	ADS3304	Exon 10/3-UTR	66.6	67.5	24.8	chr10:121099752-121099973
Zfp536	ENSMUSG00000043456	ENSMUST00000056338	ADS4510	3-Downstream	65.4	67.4	35.9	chr7:37473451-37473606
Zfp536	ENSMUSG00000043456	ENSMUST00000056338	ADS4509	Exon 4	68.4	69.9	35.4	chr7:37567973-37568130

Appendix Table 3: Target regions for each gene for methylation analysis

Method	Mean	Std dev
TPS (0.5, 6, 9.5, 19 and 28)	0.40306335962	0.2206665163
Piecewise linear over 0.5, 7, 14, 28	0.594072719494	0.399642079492
Piecewise linear over 0.5, 2, 14, 28	0.710967061349	0.721681860787
Piecewise linear over 0.5, 4, 7, 14, 28	0.560990230501	0.364739525724

Appendix Table 4: Mean and standard deviation of mean squared error over all 126 genes by *TPS* selecting 5 points and piecewise linear fits over 3 sets of points identified heuristically in the literature.

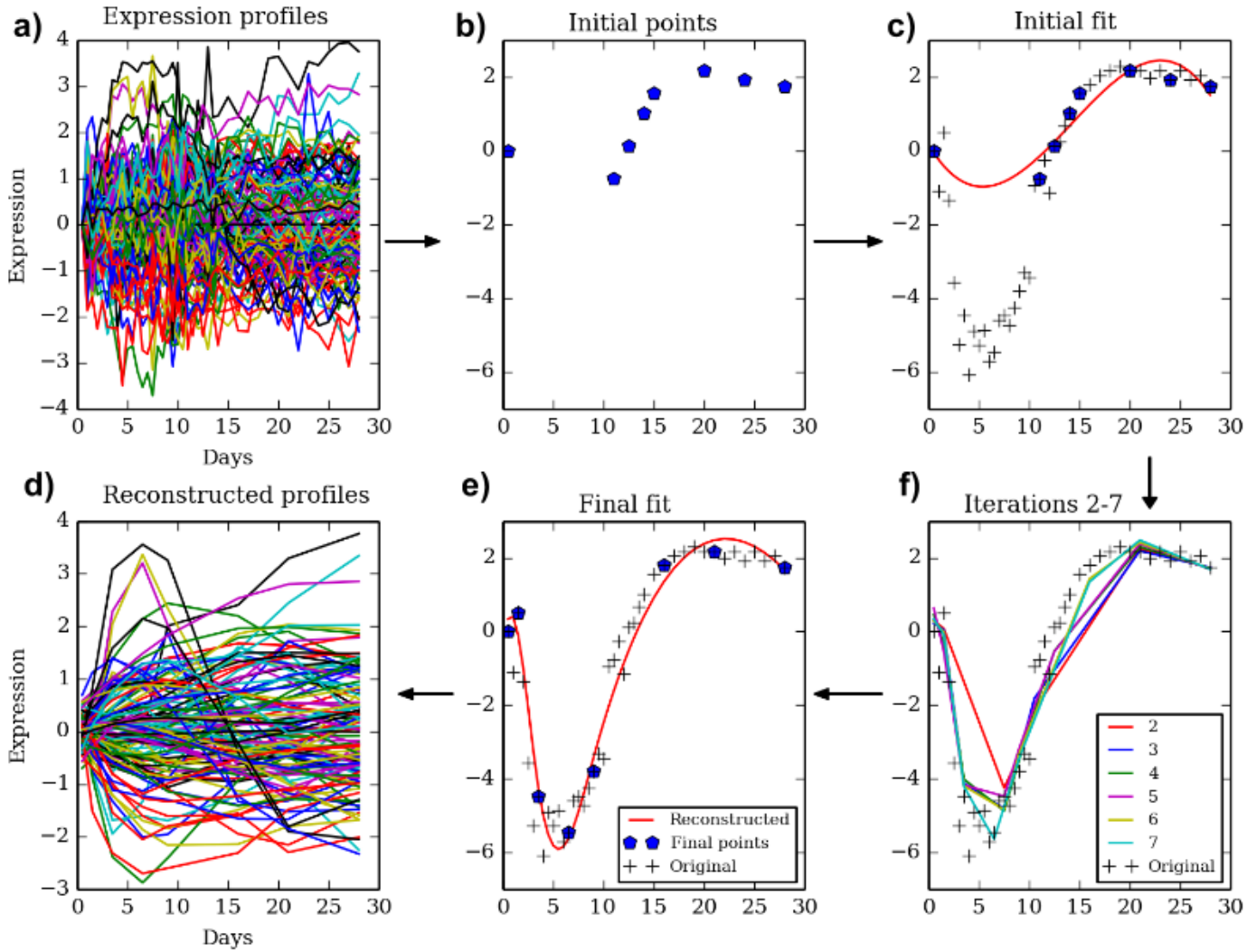
a)
Expression profiles
Expression
Days
b)
Initial points
c)
Initial fit
d)
Reconstructed profiles
Expression
Days
e)
Final fit
Reconstructed
Final points
Original
f)
Iterations 2-7
2
3
4
5
6
7
Original

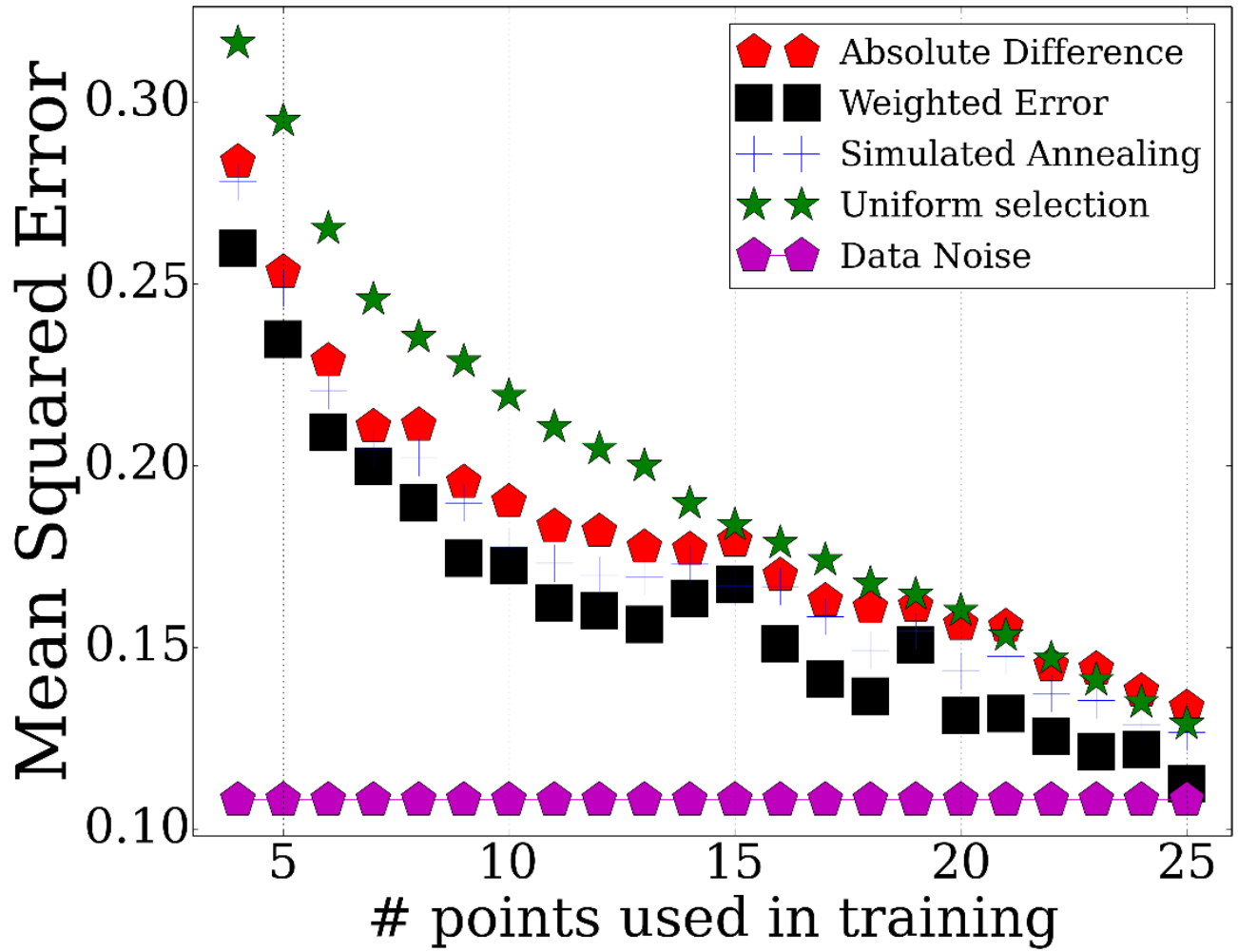
Absolute Difference
Weighted Error
Simulated Annealing
Uniform selection
Data Noise
Mean Squared Error
0.30
0.25
0.20
0.15
0.10
5
10
15
20
25
points used in training

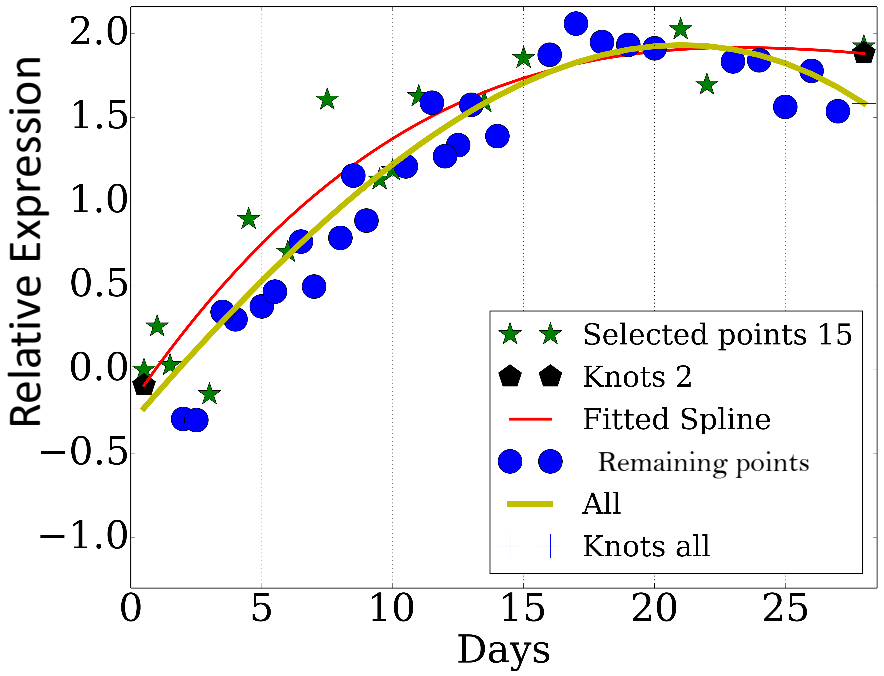

(a) *Pdgrfa*

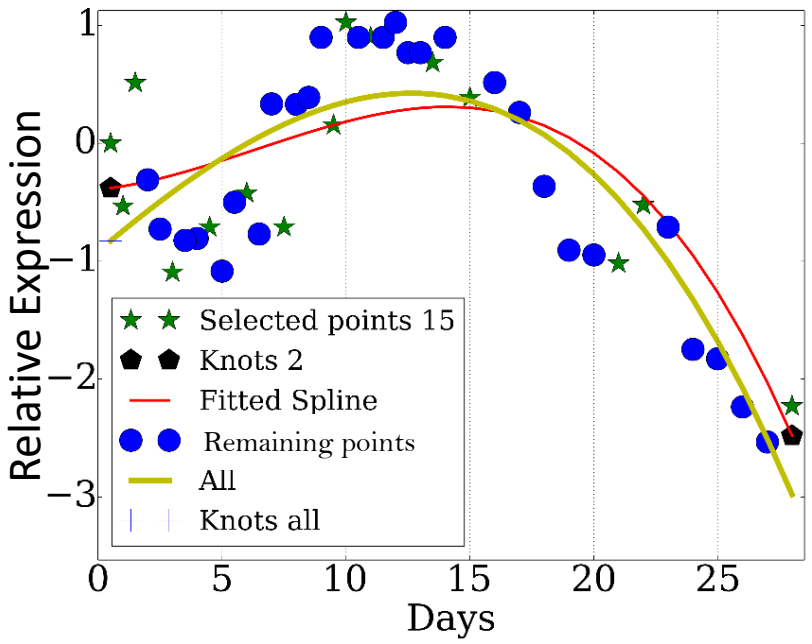

(b) *Eln*

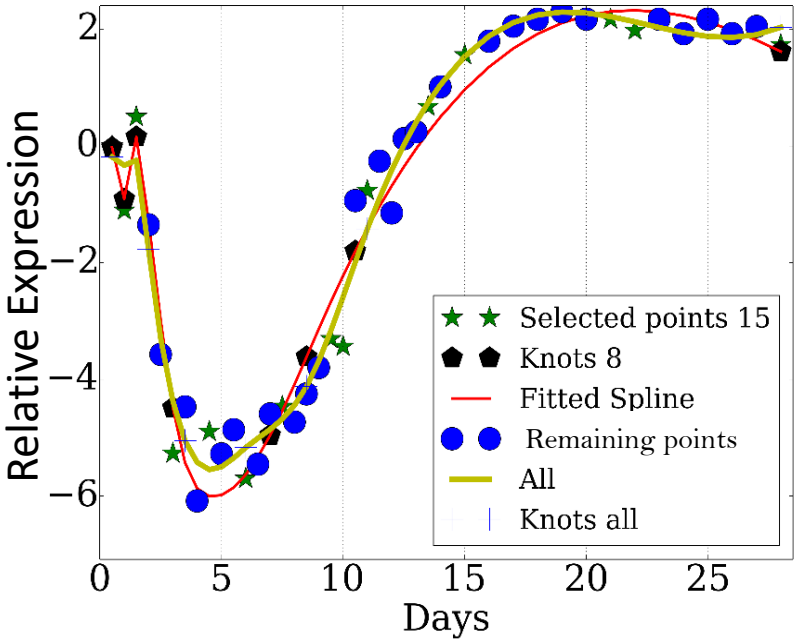

(c)*Inmt*

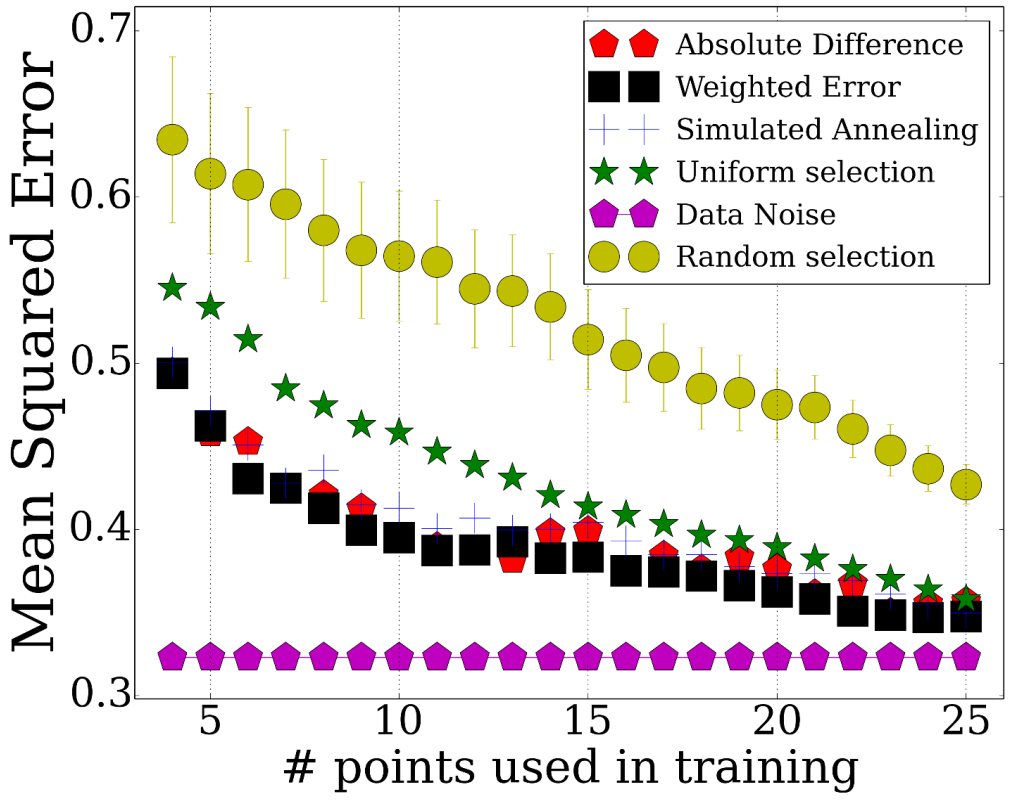
Absolute Difference
Weighted Error
Simulated Annealing
Uniform selection
Data Noise
Random selection
Mean Squared Error
0.7
0.6
0.5
0.4
0.3
5
10
15
20
25
points used in training

(a)

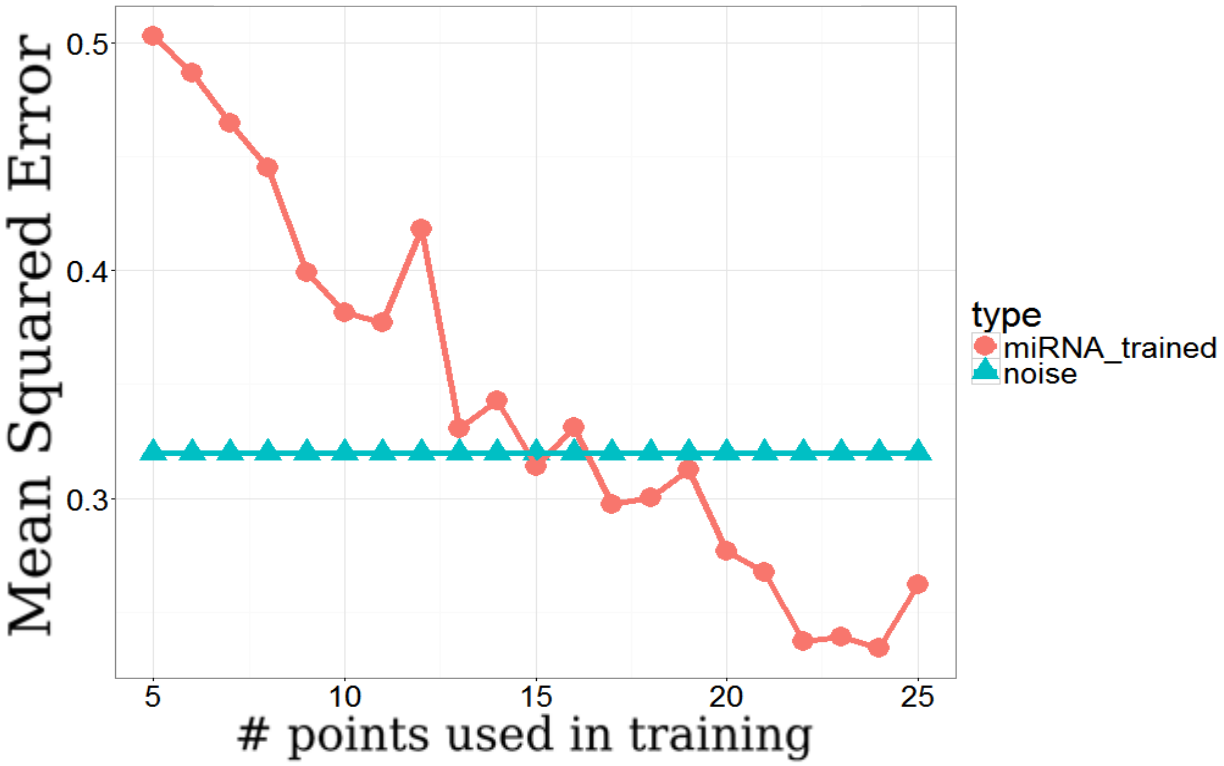
Mean Squared Error
0.5
0.4
0.3
5
10
15
20
25
points used in training
type
miRNA_trained
noise

(b)

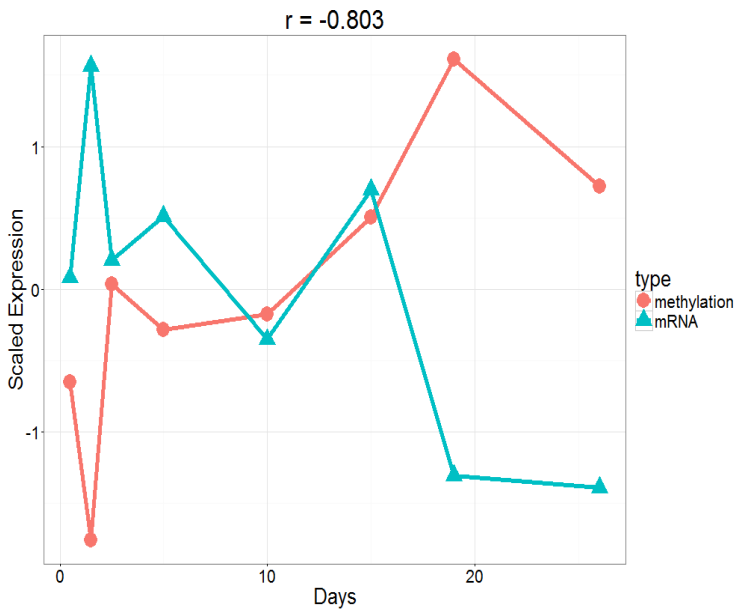

(a) *Akt1*

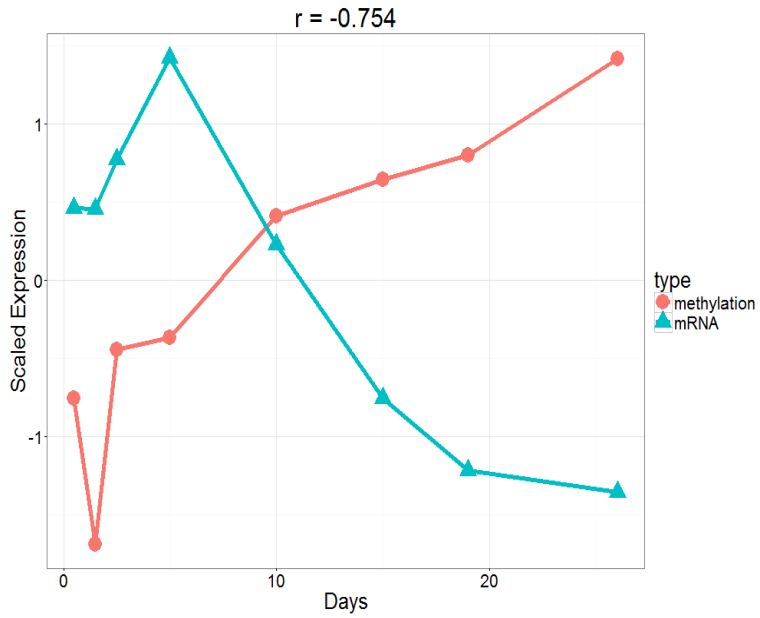

(b) *Cdh11*

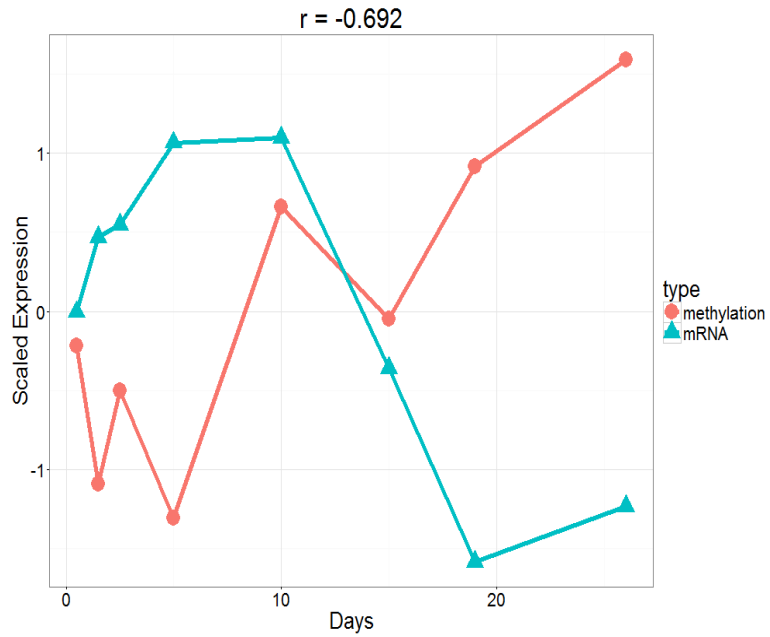

(c) *Tnc*

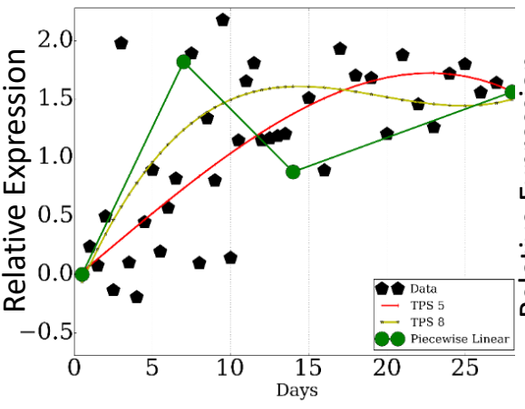

(a) *Nol3*

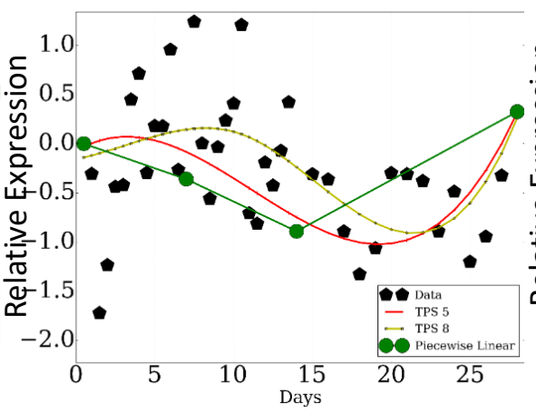

(b) *E2f8*

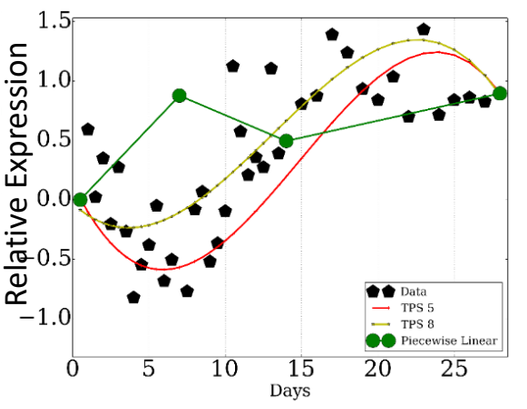

(c) *Esr2*

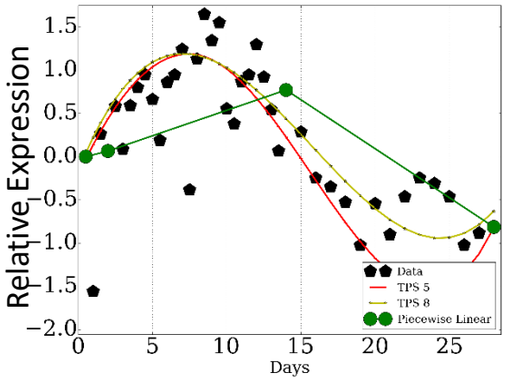

(d) *Fgf18*

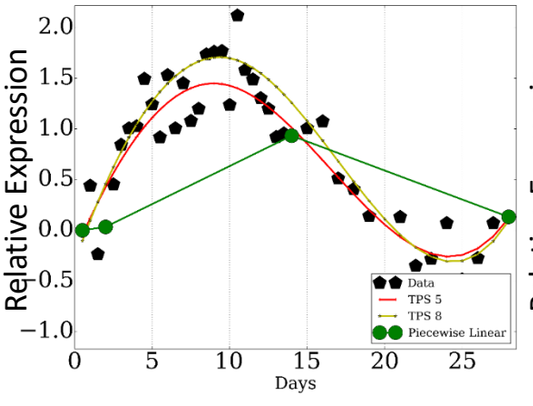

(e) *Wif1*

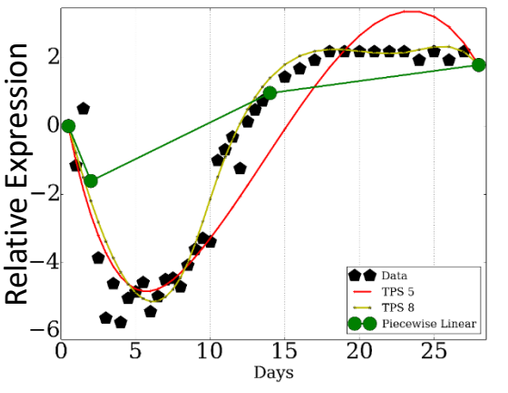

(f) *Inmt*

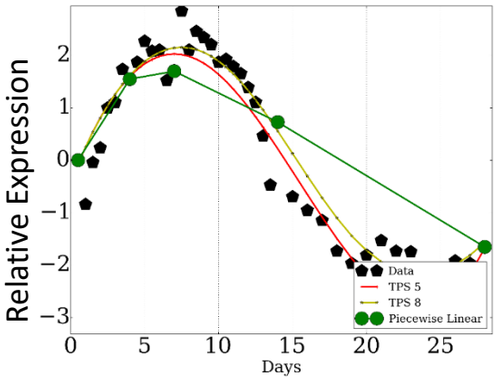

(g) *Tnc*

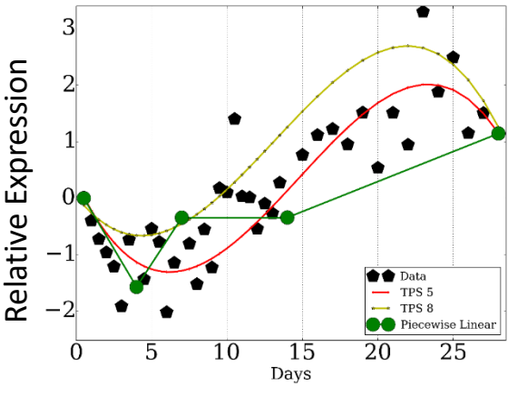

(h) *Lrat*

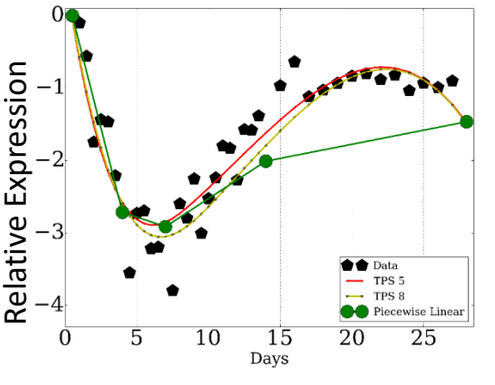

(i) *Igfpb3*

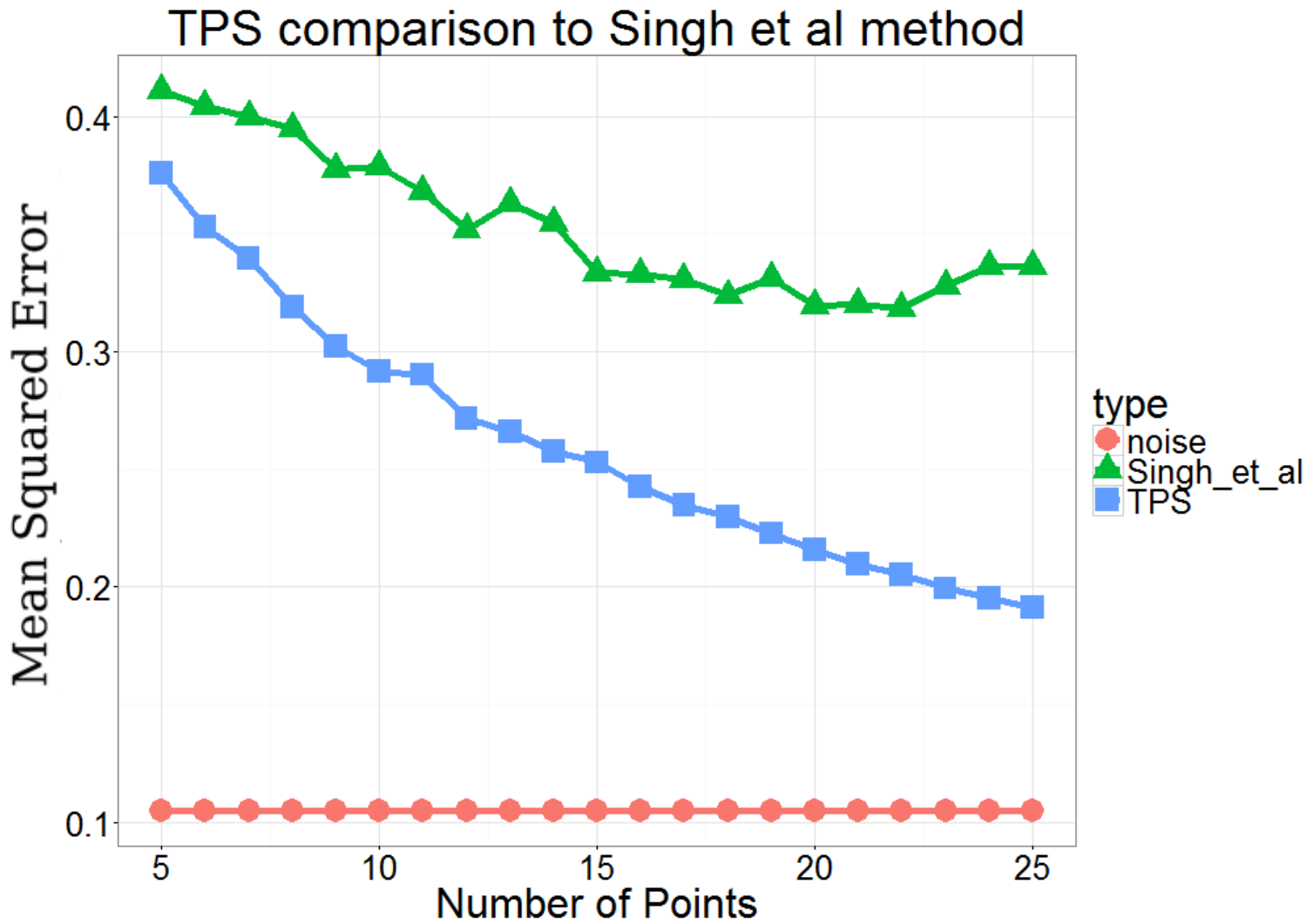
TPS comparison to Singh et al method
Mean Squared Error
0.4
0.3
0.2
0.1
5
10
15
20
25
Number of Points
type
noise
Singh_et_al
TPS

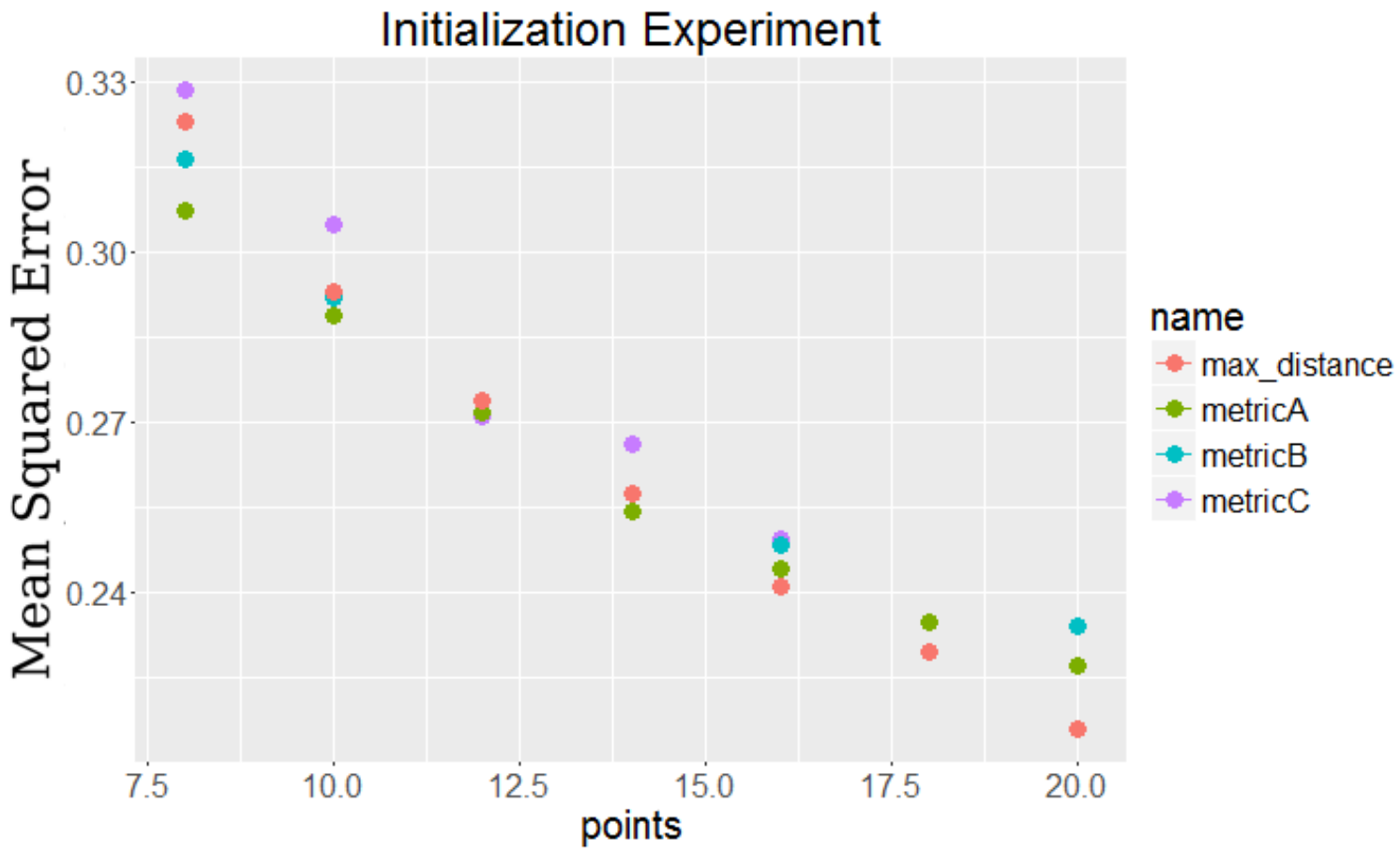
Initialization Experiment
Mean Squared Error
0.33
0.30
0.27
0.24
7.5
10.0
12.5
15.0
17.5
20.0
points
name
max_distance
metricA
metricB
metricC

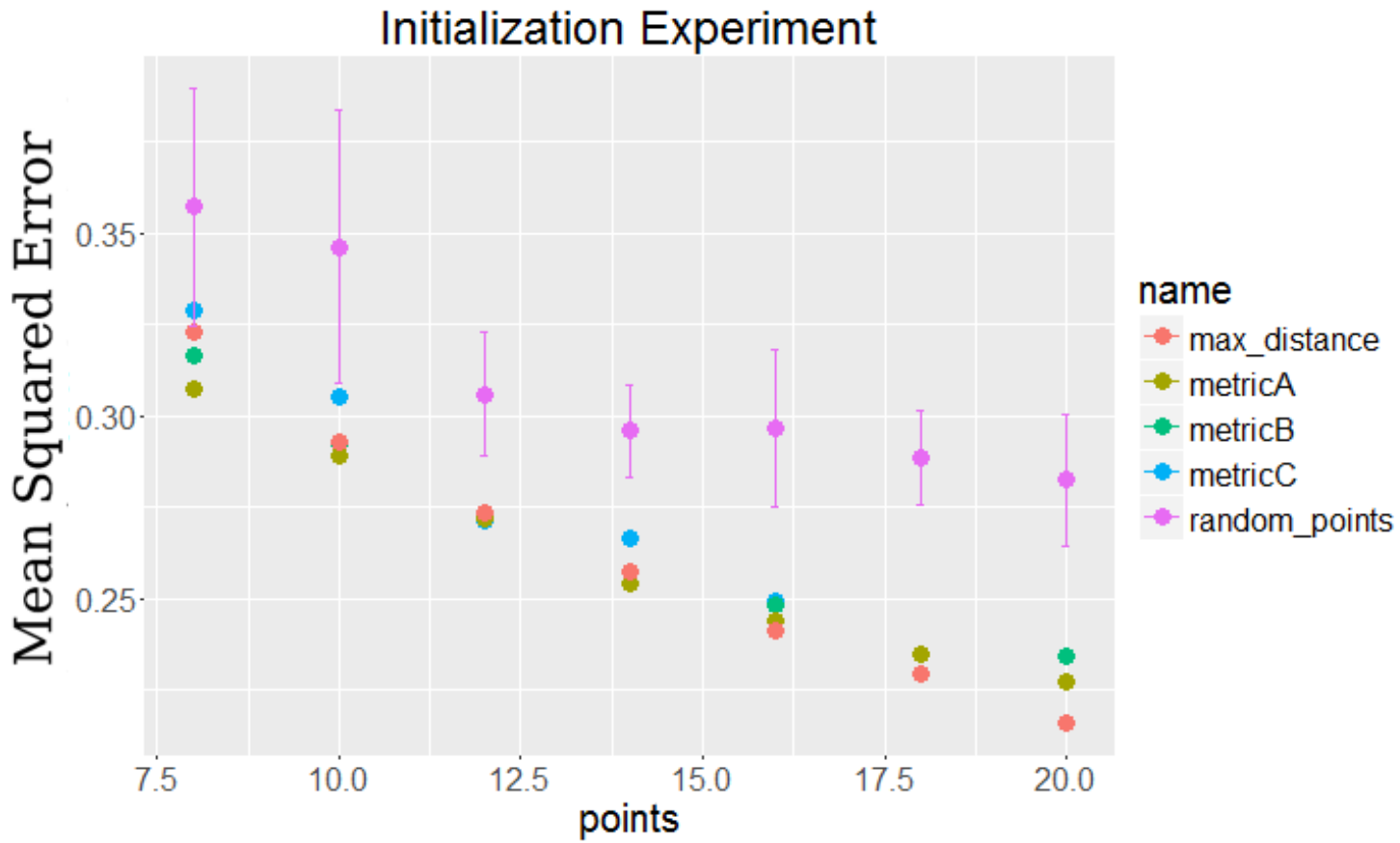
Initialization Experiment
Mean Squared Error
0.35
0.30
0.25
7.5
10.0
12.5
15.0
17.5
20.0
points
name
max_distance
metricA
metricB
metricC
random_points

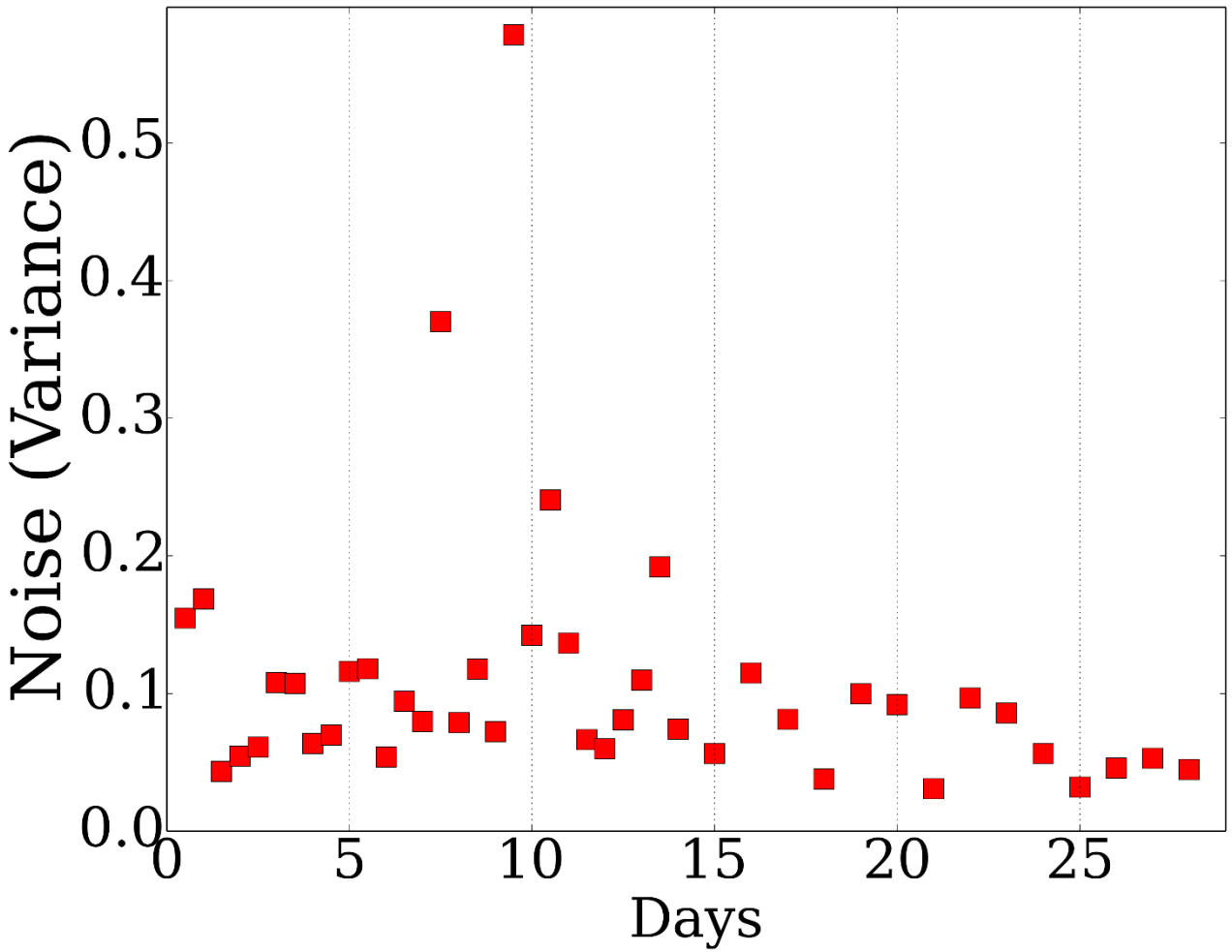
Noise (Variance)
0.0
0.1
0.2
0.3
0.4
0.5
0
5
10
15
20
25
Days

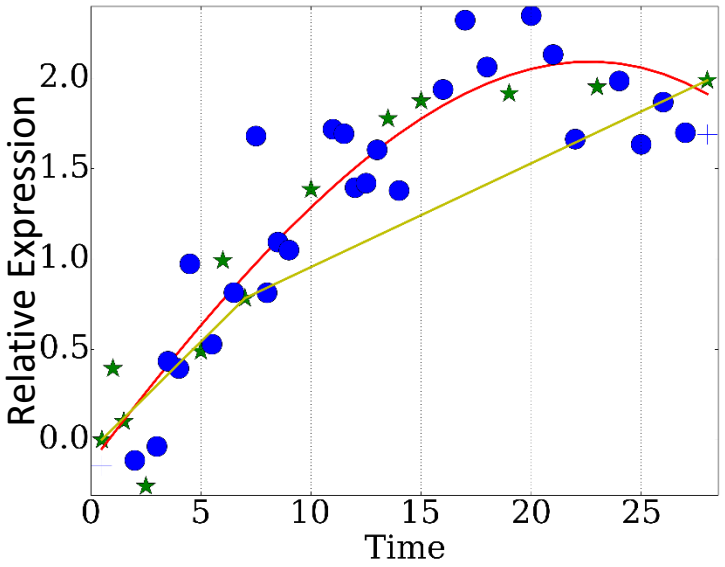

(a) *Pdgfra*

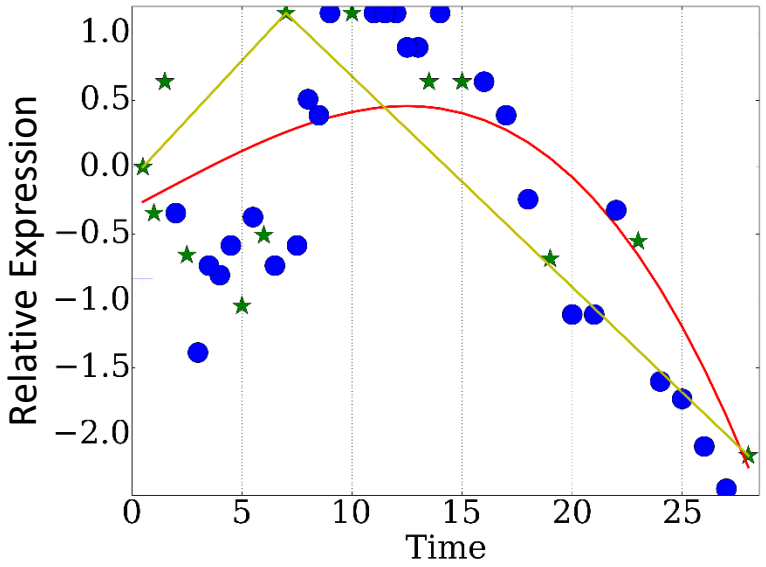

(b) *Eln*

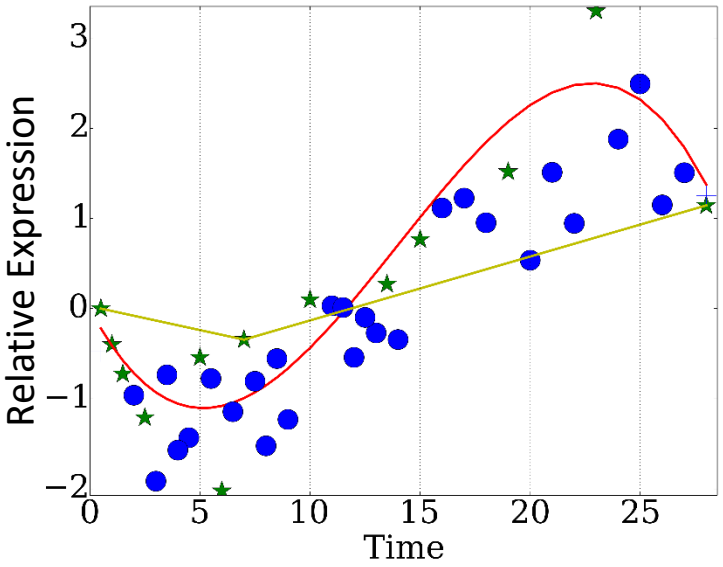

(c) *Lrat*

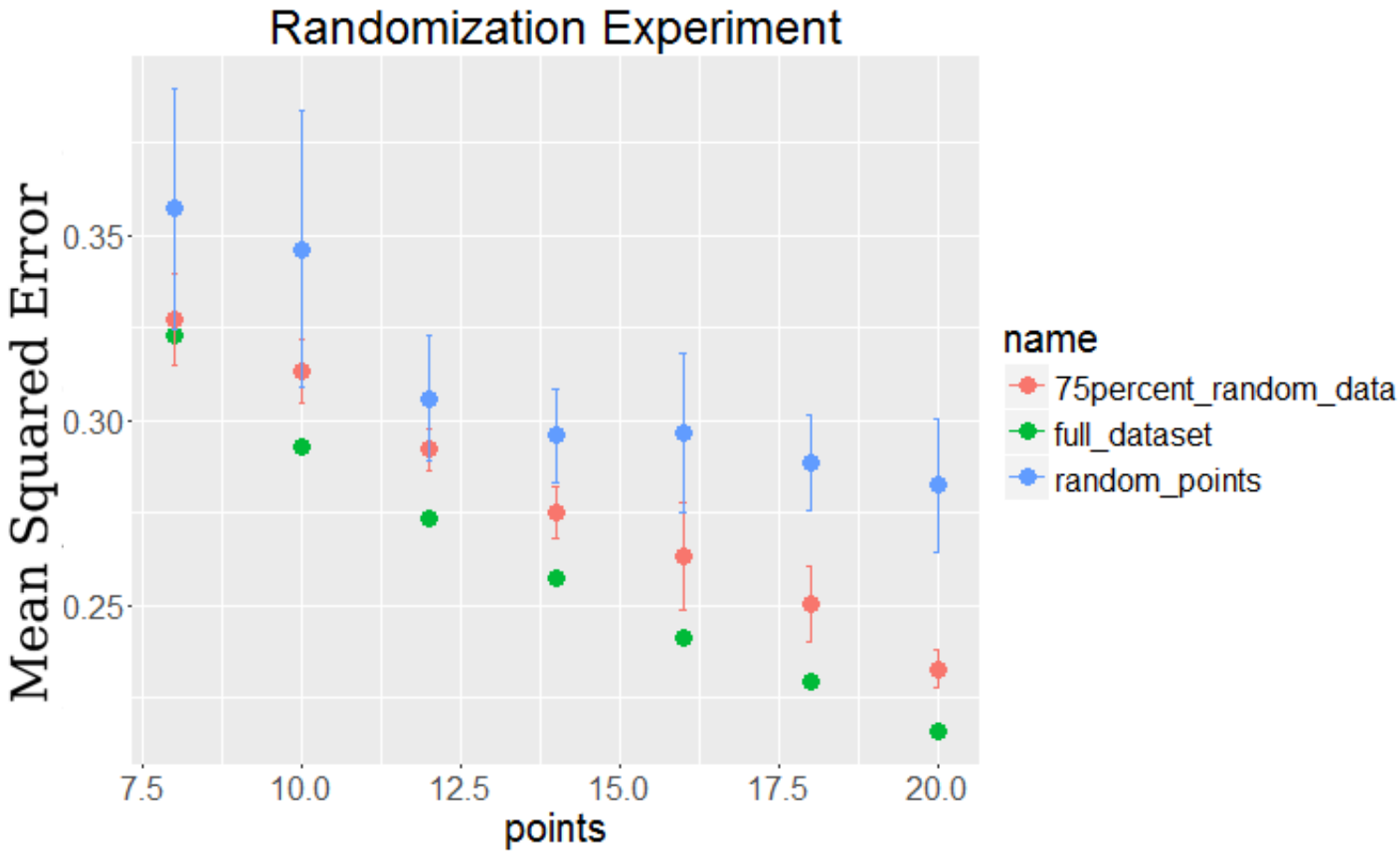
Randomization Experiment
Mean Squared Error
0.35
0.30
0.25
7.5
10.0
12.5
15.0
17.5
20.0
points
name
75percent_random_data
full_dataset
random_points

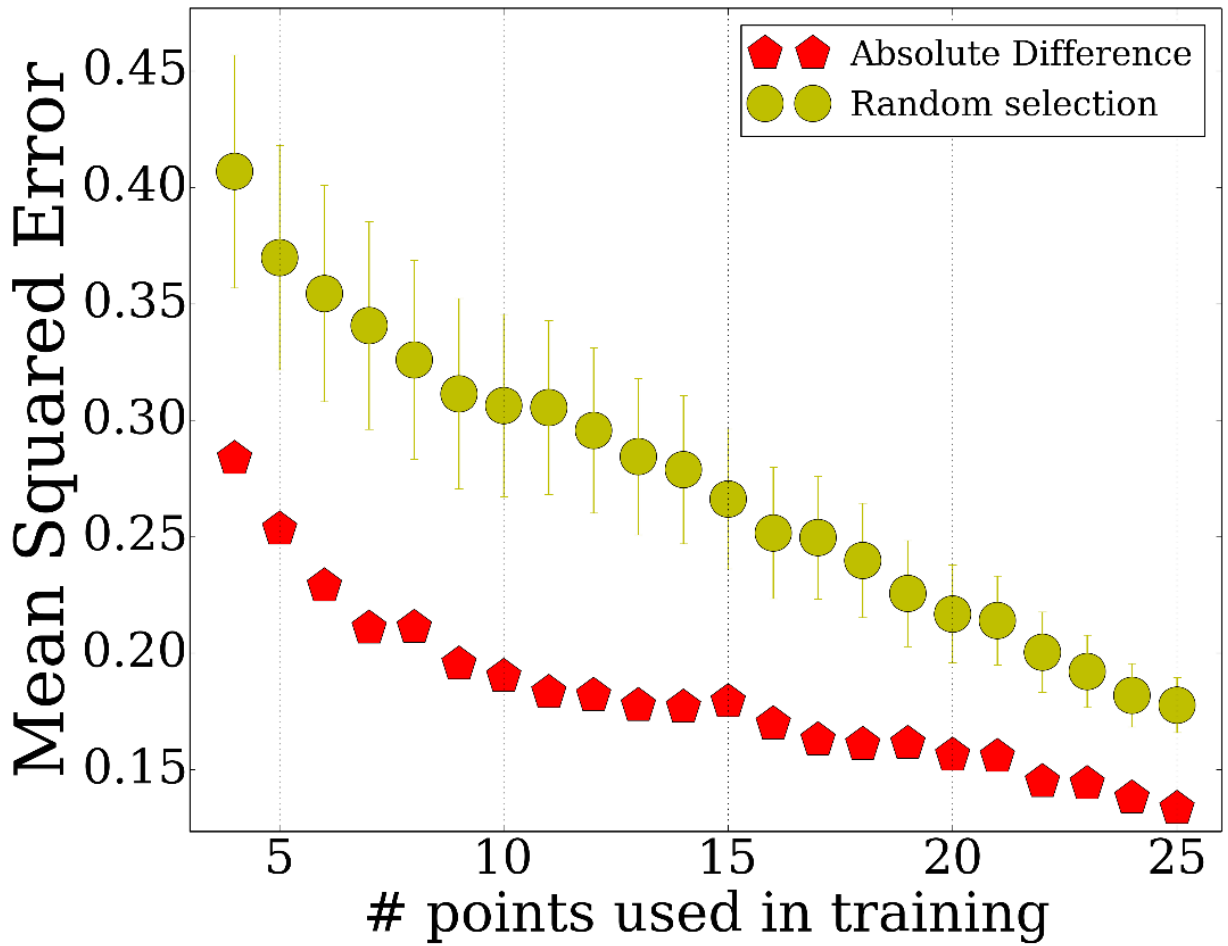
Absolute Difference
Random selection
Mean Squared Error
0.45
0.40
0.35
0.30
0.25
0.20
0.15
5
10
15
20
25
points used in training

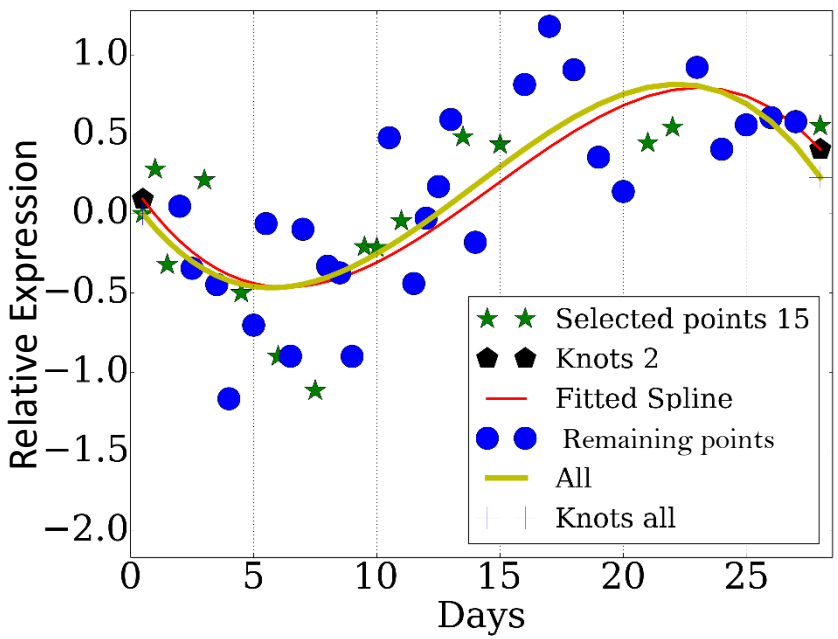

a) *Esr2*

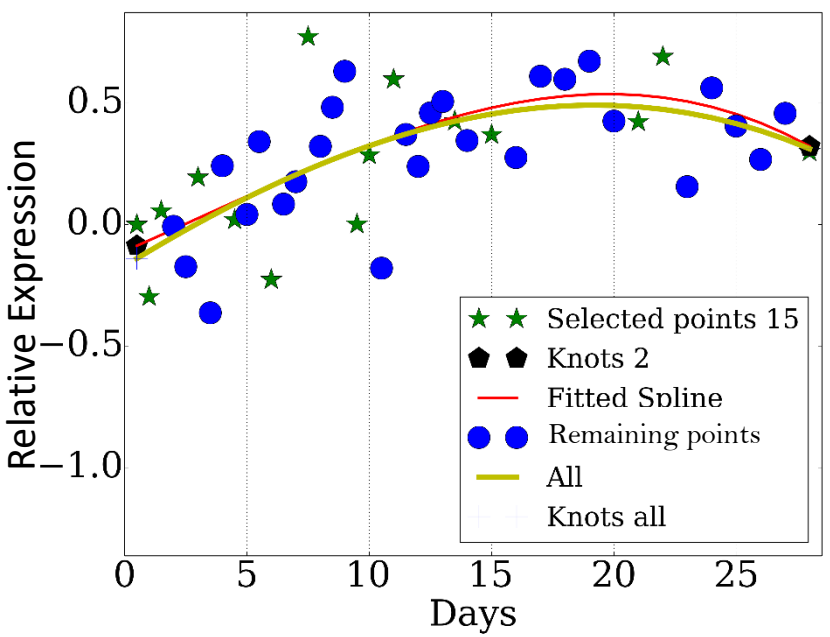

(b) *Nme3*

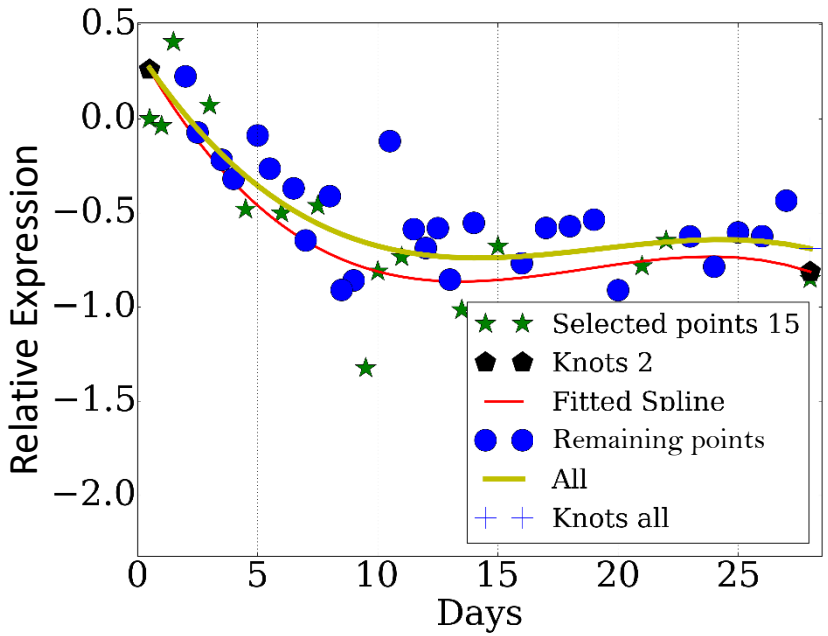

(c) *Polr2a*

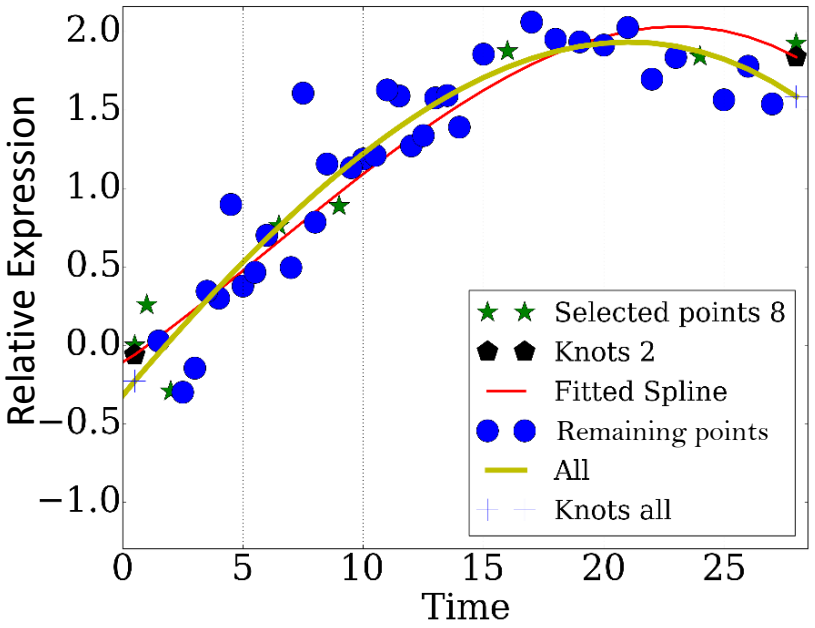

(a) *Pdgfra*

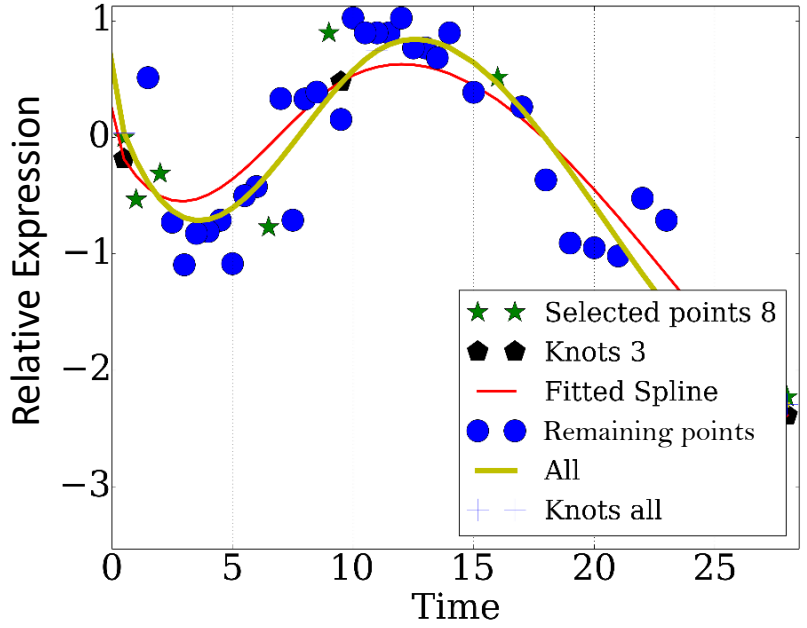

(b) *Eln*

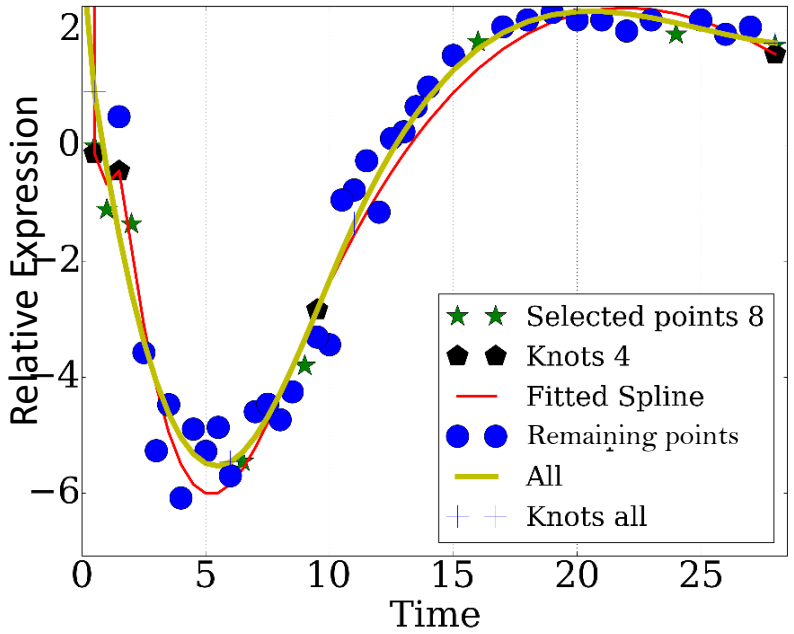

(c) *Inmt*

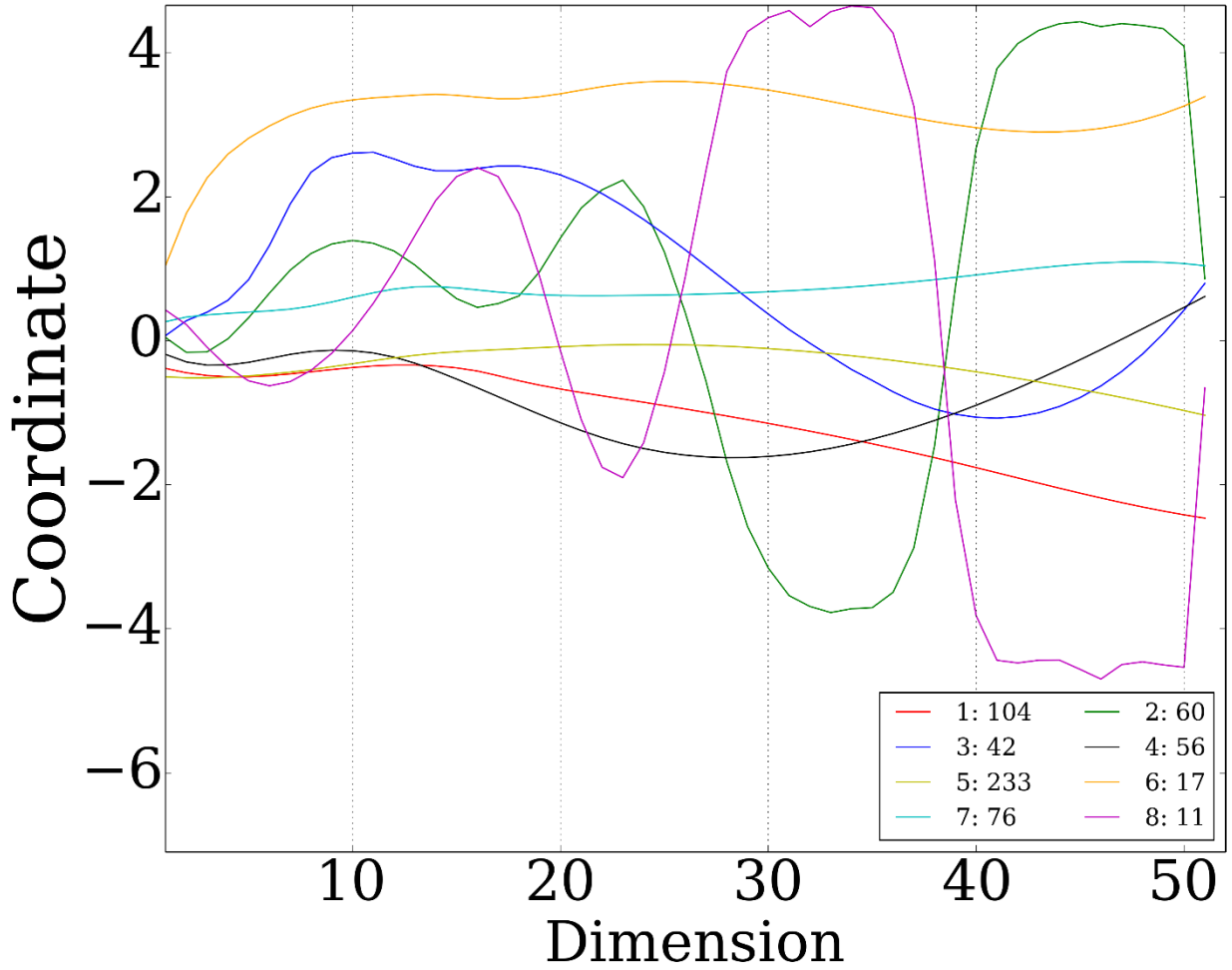
Coordinate
Dimension
4
2
0
−2
−4
−6
10
20
30
40
50
1: 104
2: 60
3: 42
4: 56
5: 233
6: 17
7: 76
8: 11

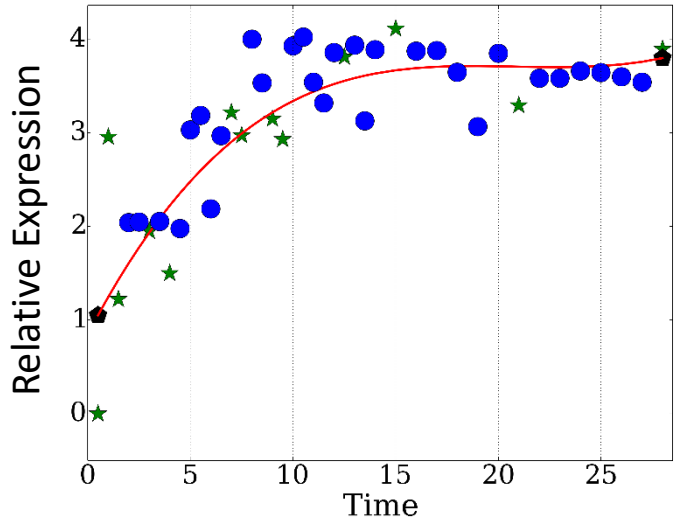

(a) *mmu-miR-100*

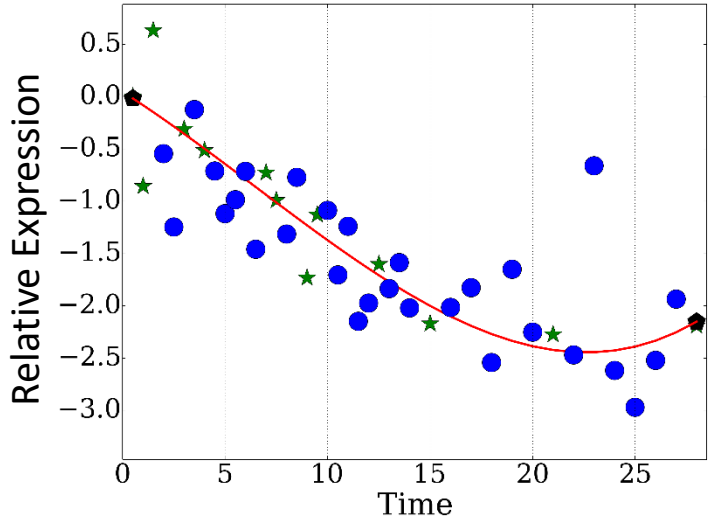

(b) *mmu-miR-136*

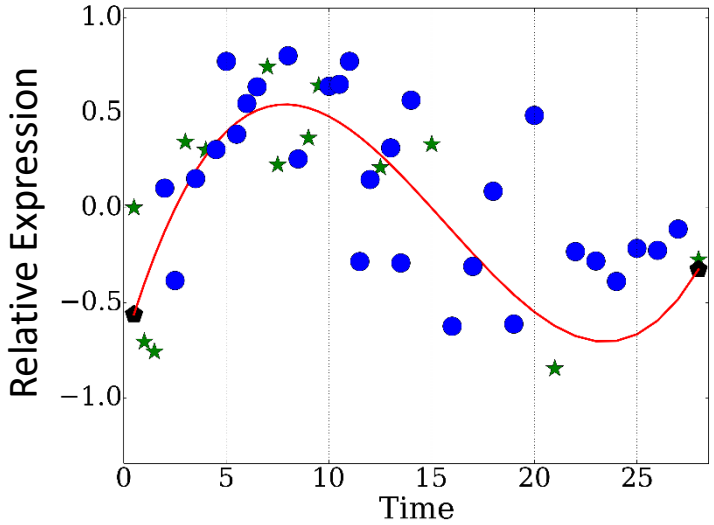

(c) *mmu-miR-152*

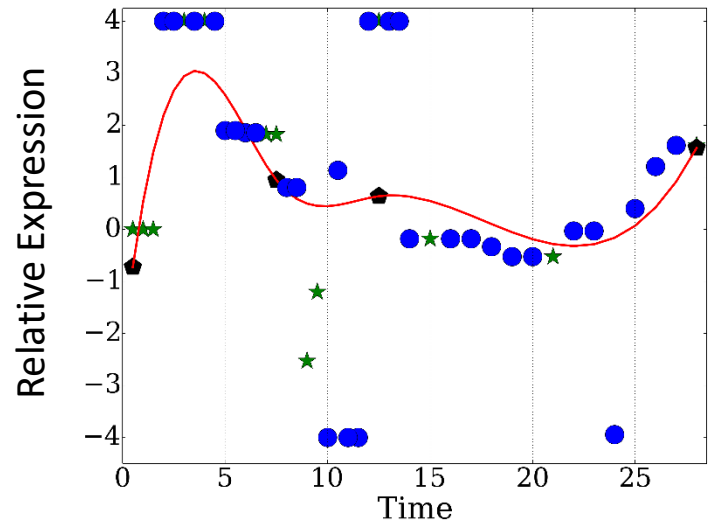

(d) *mmu-miR-219*

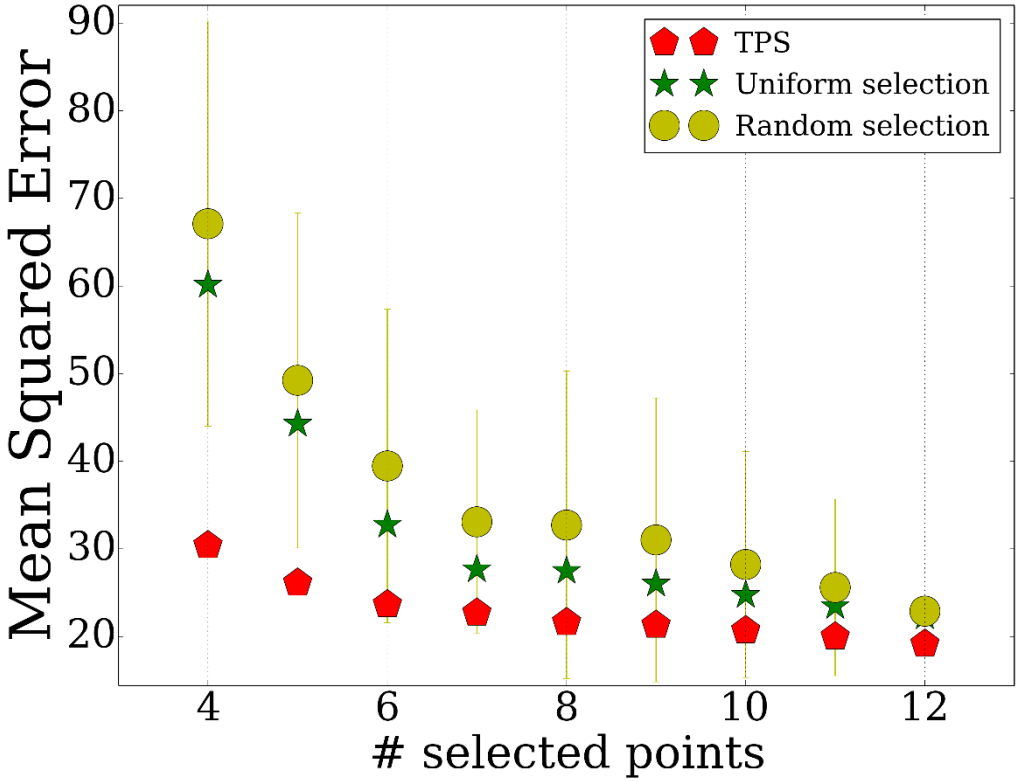
Mean Squared Error
90
80
70
60
50
40
30
20
4
6
8
10
12
selected points
TPS
Uniform selection
Random selection

(a)

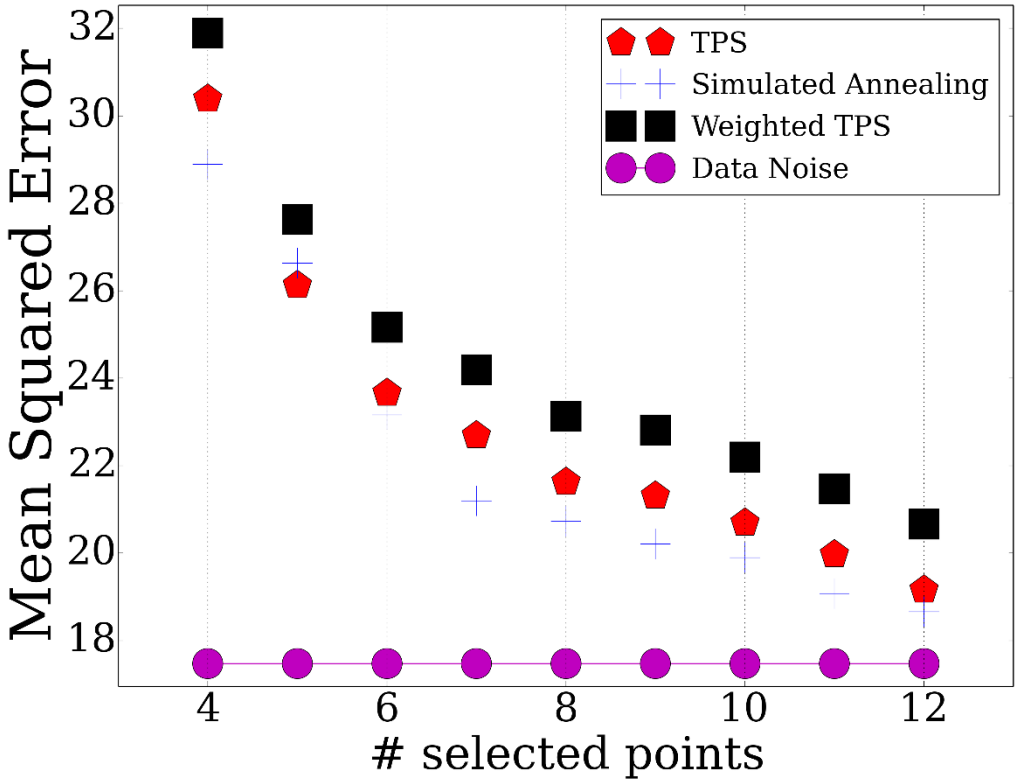
Mean Squared Error
32
30
28
26
24
22
20
18
4
6
8
10
12
selected points
TPS
Simulated Annealing
Weighted TPS
Data Noise

(b)

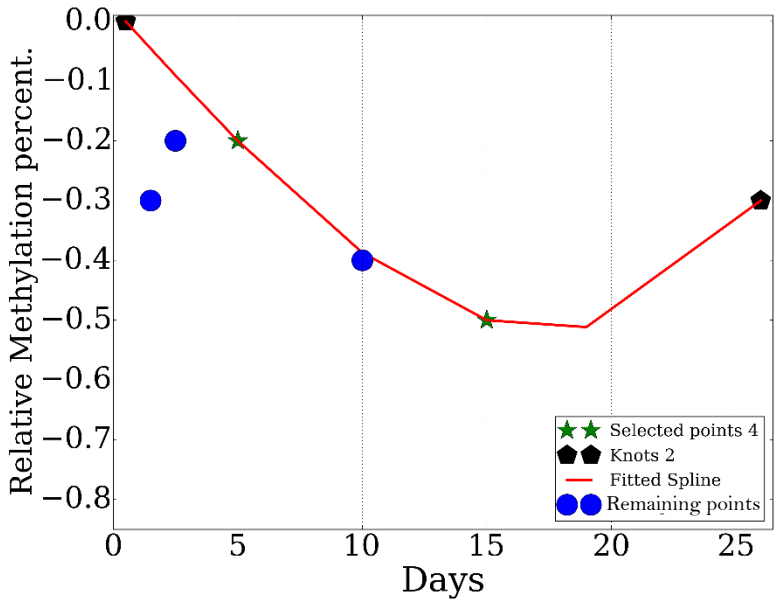

(a) Chrom. 2, 157423995 (*Src*)

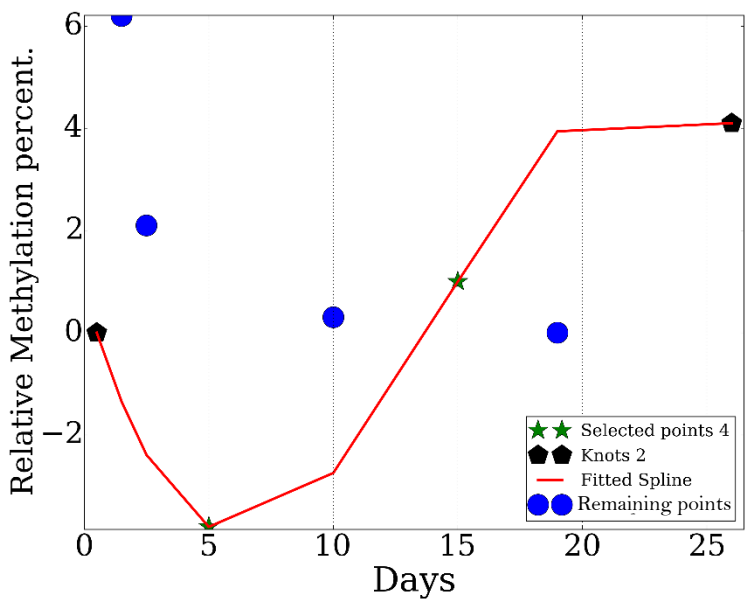

(b) Chrom. 5, 134721315 (*Eln*)

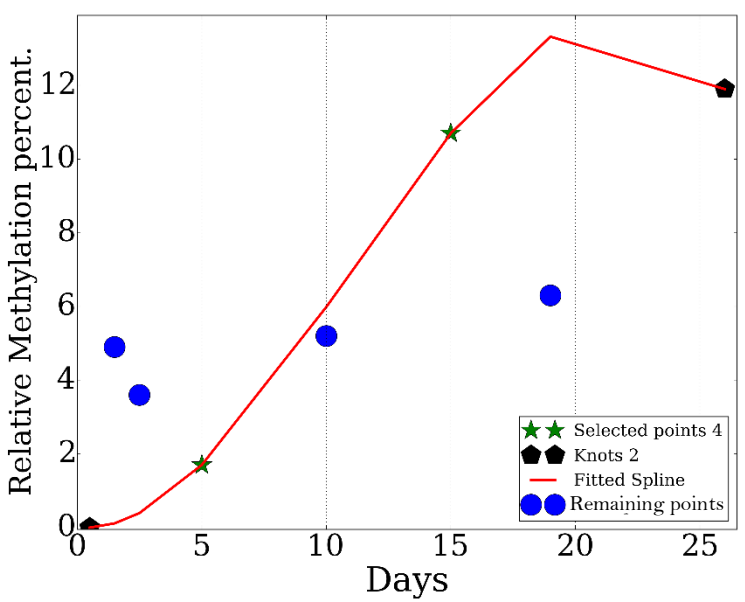

(c) Chrom. 12, 112657170 (*Akt1*)

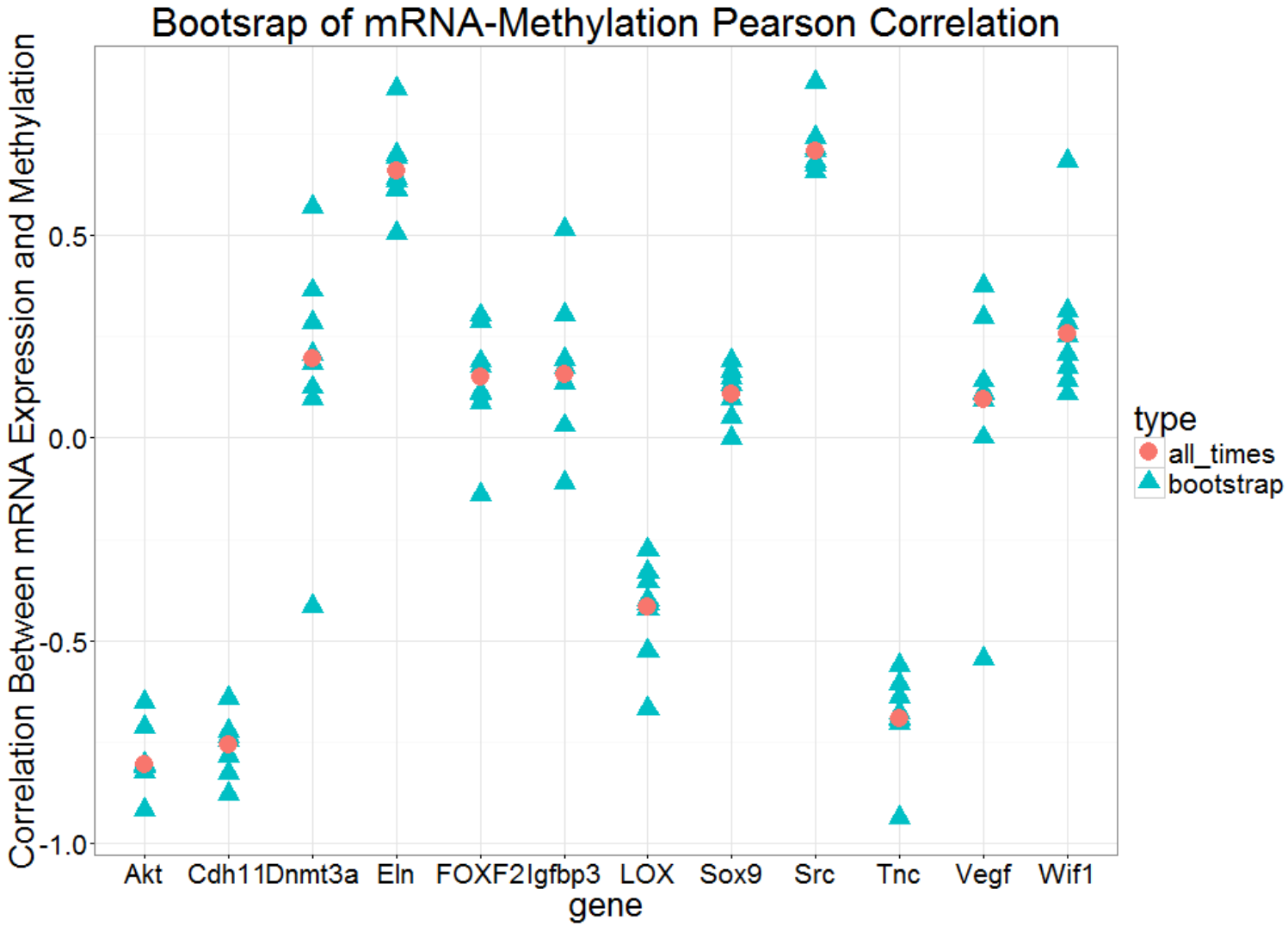
Bootsrap of mRNA-Methylation Pearson Correlation
Correlation Between mRNA Expression and Methylation
0.5
0.0
-0.5
-1.0
Akt
Cdh11
Dnmt3a
Eln
FOXF2
Igfbp3
LOX
Sox9
Src
Tnc
Vegf
Wif1
gene
type
all_times
bootstrap

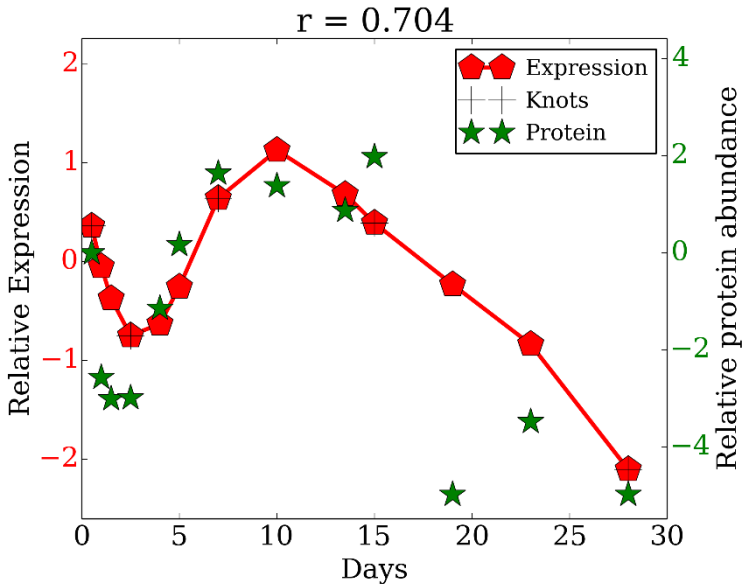

(a) *Eln / P54320*

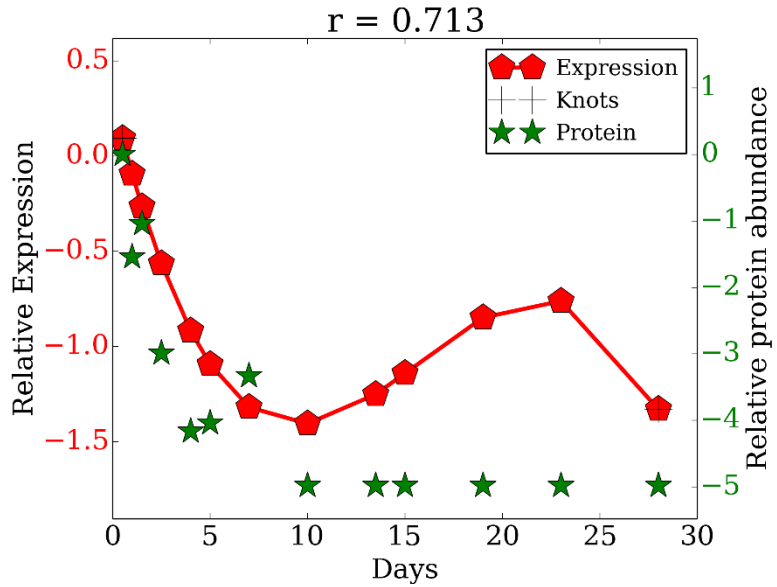

(b) *F13a1 / Q8BH61*

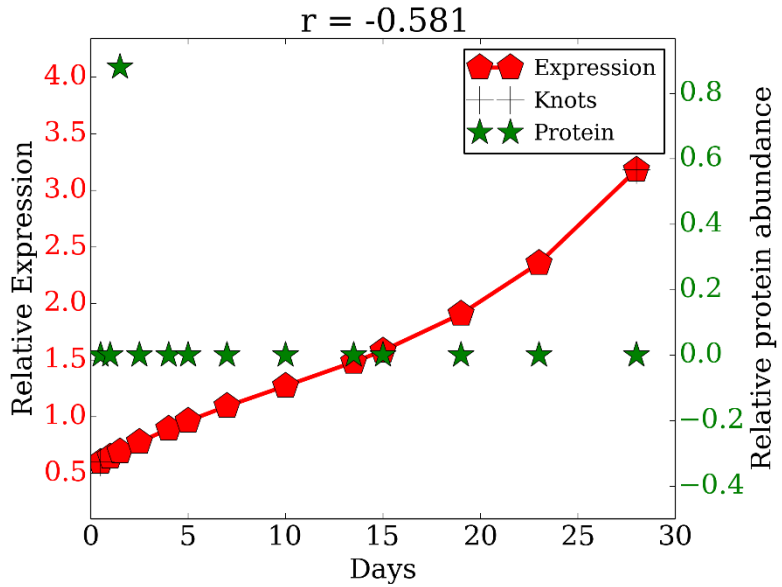

(c) *Chi3l1 / Q61362*.